Appl Microbiol Biotechnol (2014) 98:9777–9794
DOI 10.1007/s00253-014-6040-9

APPLIED MICROBIAL AND CELL PHYSIOLOGY

Chemostat cultivation and transcriptional analyses of *Clostridium acetobutylicum* mutants with defects in the acid and acetone biosynthetic pathways

Daniel Hönicke · Tina Lütke-Eversloh · Ziyong Liu · Dörte Lehmann · Wolfgang Liebl · Armin Ehrenreich

Received: 13 March 2014 / Revised: 13 August 2014 / Accepted: 20 August 2014 / Published online: 4 October 2014

Abstract *Clostridium acetobutylicum* is a model organism for the biotechnologically important acetone–butanol–ethanol (ABE) fermentation. With the objective to rationally develop strains with improved butanol production, detailed insights into the physiological and genetic mechanisms of solvent production are required. Therefore, pH-controlled phosphate-limited chemostat cultivation and DNA microarray technology were employed for an in-depth analysis of knockout mutants with defects in the central fermentative metabolism. The set of studied mutants included strains with inactivated phosphotransacetylase (*pta*), phosphotransbutyrylase (*ptb*), and acetoacetate decarboxylase (*adc*) encoding genes, as well as an *adc*/*pta* double knockout mutant. A comprehensive physiological characterization of the mutants was performed by continuous cultivation, allowing for a well-defined separation of acidogenic and solventogenic growth, combined with the advantage of the high reproducibility of steady-state conditions. The *ptb*-negative strain *C. acetobutylicum ptb*::int(87) exhibited the most striking metabolite profile: Sizable amounts of butanol (29±1.3 mM) were already produced during acidogenic growth. The product patterns of the mutants as well as accompanying transcriptomic data are presented and discussed.

Keywords Biofuel · Biobutanol · ClosTron · Chemostat cultivation · DNA microarray

D. Hönicke · Z. Liu · W. Liebl · A. Ehrenreich (✉)
Lehrstuhl für Mikrobiologie, Technische Universität München, Emil-Ramann Straße 4, 85354 Freising, Germany
e-mail: aehrenr@mikro.biologie.tu-muenchen.de

T. Lütke-Eversloh (✉) · D. Lehmann
Abteilung Mikrobiologie, Institut für Biowissenschaften, Universität Rostock, Albert-Einstein-Str. 3, 18059 Rostock, Germany
e-mail: tina.luetke-eversloh@uni-rostock.de

Present Address:
Z. Liu
Key Laboratory of Biofuels, Qingdao Institute of Bioenergy and Bioprocess Technology, Chinese Academy of Sciences, Qingdao 266101, China

Introduction

The Gram-positive, strict anaerobic endospore-forming bacterium *Clostridium acetobutylicum* with its acetone–butanol–ethanol (ABE) fermentative metabolism has become a model organism to study the unique physiology of solventogenic clostridia. In typical batch fermentations, *C. acetobutylicum* produces the organic acids acetate and butyrate along with molecular hydrogen during exponential growth, commonly designated as acidogenesis. The transition to the stationary growth phase is characterized by a metabolic shift to solventogenesis in which parts of the previously excreted acids are re-assimilated and the neutral ABE solvents are produced, typically at a ratio of 3:6:1 (Berezina et al. 2012; Jones and Woods 1986; Lee et al. 2008).

The most desired product of ABE fermentation is *n*-butanol, which is an attractive renewable liquid fuel with several advantages over ethanol (Green 2011; Jin et al. 2011). The major drawback of the ABE fermentation process is the relatively low butanol yield, due to by-product formation and the toxicity of butanol to the cells (Ezeji et al. 2010; Liu and Qureshi 2010). In order to improve the butanol titer, yield, and productivity, various strategies have been applied to increase the metabolic flux towards *n*-butanol synthesis in solventogenic clostridia (Jang et al. 2012a; Lütke-Eversloh and Bahl 2011; Papoutsakis 2008). However, despite many decades of research, relatively little is known about the key metabolic steps and their underlying regulatory circuits triggering the shift from acidogenesis to solventogenesis, mostly

because no sufficient tools for molecular biology were available for clostridia (Lütke-Eversloh 2014). Downregulation of genes by antisense RNA technology (Desai and Papoutsakis 1999; Tummala et al. 2003) or gene knockout using single crossover recombination (Green and Bennett 1996; Green et al. 1996; Sillers et al. 2008; Nair et al. 1999) showed only limited success. Thus, traditional defective mutant analyses could not be exhaustively conducted until the group II intron-based ClosTron technique became available as a reliable and reproducible system for targeted mutagenesis in clostridial species (Heap et al. 2007, 2010).

Although a number of *C. acetobutylicum* mutants with defects in several branch pathways of the central metabolism were constructed, a comprehensive understanding of how the network of acid re-assimilation and solvent formation is controlled has not yet been achieved. Usually, the phenotypes of these mutants were characterized in batch cultures with quantification of metabolites during the course of fermentation (Cooksley et al. 2012; Jang et al. 2012b; Lehmann et al. 2012a). These data provided valuable information about the global metabolic effects caused by each mutation, but major aspects of the phenotype are often not visible in batch cultures because many parameters such as the substrate and product concentrations change or the cells undergo differentiation during cultivation. Continuous cultivation on the other hand allows a clearly defined separation of acidogenic and solventogenic growth by changing only the pH of the culture, resulting in constant internal and external parameters when steady states have been reached (Bahl et al. 1982; Tashiro et al. 2013). Moreover, studies on continuous cultures have clearly indicated that solventogenesis is independent from sporulation (Grimmler et al. 2011). Thus, continuous cultures generate highly reproducible data for comparative transcriptomic, proteomic, or metabolomic studies allowing new insights in metabolic details of acidogenesis and solventogenesis as well as the transition between these metabolic states under standardized conditions (Grimmler et al. 2011; Janssen et al. 2010).

In this study, we used a pH-controlled phosphate-limited chemostat to physiologically characterize ClosTron-mediated knockout mutants of *C. acetobutylicum* ATCC 824 with defects in the butyrate, acetate, and acetone biosynthetic pathways, as well as a combination of the latter two. The metabolite profiles of the mutants revealed accordance with previous results from batch fermentation experiments on one hand and important new observations on the other hand. Furthermore, the data derived from steady-state conditions allow conclusions to be drawn about the acid re-assimilation pathways in *C. acetobutylicum*. Genome-wide DNA microarray analyses of all mutants were conducted using the wild-type strain ATCC 824 as reference.

Materials and methods

Bacterial strains and cultivation conditions

The wild-type strain *C. acetobutylicum* ATCC 824 and four derived mutants, *C. acetobutylicum* phosphotransbutyrylase (*ptb*)::int(87) (CAC3076), phosphotransacetylase (*pta*)::int(80) (CAC1742), acetoacetate decarboxylase (*adc*)::int(180) (CAP0165), and the double knockout strain *adc*::int(180)ΔRAM-*pta*::int(80), were used in this study. ClosTron mutagenesis and genotypic verification of the strains were described in detail previously (Lehmann et al. 2012a, b). The correct intron insertions were controlled by PCR with gene- and intron-specific primers according to Lehmann et al. (2012a, b).

Clostridium strains were stored at −70 °C as spore suspension in Mineral Salt Medium (MS-MES) (Hillmann et al. 2008) or in clostridial growth medium (CGM) (Roos et al. 1985; Wiesenborn et al. 1988) with 10 % glycerol. CGM precultures (5 ml) inoculated with spores were pasteurized for 10 min at 80 °C to inactivate vegetative cells prior to cultivation under anaerobic conditions at 37 °C overnight in Hungate tubes (Ochs GmbH, Bovenden, Germany). Phosphate-limited continuous culture experiments were performed at 37 °C in a Biostat B*plus* 1-L fermentor system (Sartorius BBI Systems, Melsungen, Germany) with a working volume of 0.75 L in a medium containing 0.5 mM KH_2PO_4 and 4 % (*w*/*v*) glucose (Grimmler et al. 2011). The dilution rate was adjusted to $D = 0.075\ h^{-1}$ and the pH was controlled by the automatic addition of 2 M KOH. Inoculation, addition, and sample drawing were conducted using disposable plastic syringes purchased from Medi-King (Oyten, Germany).

Analytical methods

Cell growth was monitored by measuring the optical density at 600 nm (OD_{600}). The concentrations of butyrate, acetate, ethanol, acetone, and butanol in cell-free supernatant samples were measured by gas chromatography (GC-2010, Shimadzu, Duisburg, Germany) using a Stabilwax-DA column according to the method of Thormann et al. (2002). Glucose and lactate in culture supernatants were determined with GOPOD and D-/L-lactic acid kits according to instructions of the supplier (Megazyme, Wicklow, Ireland).

DNA microarray experiments

Isolation of total RNA and DNase treatment was performed as previously described (Grimmler et al. 2011). DNA-free RNA aliquots were transcribed into Cy3- or Cy5-labeled cDNA. Dye swaps with reverse-labeled samples were done to exclude dye-specific effects. Microarray experiments were usually reproduced and representative data are given. cDNA labeling,

hybridization, DNA chips used, data normalization (GenePix Pro 6.0 software), and correction were described in detail by Grimmler et al. (2011). A threshold of 3 was used to define significantly upregulated (≥3.0) or repressed (≤−3.0) genes. Microarray data were deposited in the ArrayExpress database (www.ebi.ac.uk/arrayexpress) under the accession number E-MTAB-2058.

Results

Disruption of the acetate and acetone pathways

Continuous cultures and product patterns

In an attempt to improve the carbon flux towards *n*-butanol synthesis, we previously constructed a pta-negative *pta*::int(80) mutant using the ClosTron technology. However, batch cultivation experiments in a defined mineral salts medium revealed that its phenotype was quite similar to that of the wild type (Lehmann et al. 2012a). In order to achieve a better characterization of this mutant, it was cultivated in a phosphate-limited continuous culture. After 4 days (t=96 h), a constant cell density of OD_{600} ~4 and stable product concentrations (acetate ~5 mM, butyrate ~95 mM) marked the beginning of acidogenic steady-state growth at pH 5.7. The *pta*::int(80) mutant produced ~5 mM acetate versus ~31 mM in the wild type and showed a significantly increased butyrate formation of ~95 mM in comparison to the wild type (~57 mM). Sampling for DNA microarray analysis took place 24 h later (t=120 h). Subsequently, the pH regulation was temporarily turned off, and the pH decreased within 21 h solely by the cells' acidification of the medium to pH 4.5, which was about 12.5 h longer than the pH shift of the wild type. Solventogenic steady-state growth was reached within 24 h after the pH control was re-started at pH 4.5. The glucose concentration in the supernatant of the *pta* mutant increased to ~94 mM, which was much higher than in the wild type (~69 mM) and the OD_{600} remained stable at ~3.7 (Fig. 1b). With respect to the wild-type strain, comparable amounts of butanol (~37 mM) and acetone (~18 mM), as well as low amounts of ethanol (~3 mM), were produced during steady-state solventogenic growth. Furthermore, a constant butyrate concentration of ~19 mM was measured, which was comparable to the titer of the reference strain (~24 mM).

Since acetone constitutes the major unwanted by-product for biobutanol production, disruption of the acetone biosynthetic pathway was one of the first metabolic engineering targets (Jiang et al. 2009; Tummala et al. 2003). Hence, using the ClosTron system, the acetoacetate decarboxylase gene *adc* was knocked out by generating a *adc*::int(180) mutant. This strain showed a clear low-acetone phenotype with concomitantly elevated acetate levels in batch cultures (Lehmann et al. 2012a). In the present study, the metabolite profiles and transcriptional patterns of the *adc* mutant were analyzed using stable pH-controlled chemostat cultures. Acidogenic steady-state growth was reached after 4 days (t=96 h) as shown by a stable OD_{600} of 4.51, as well as constant glucose (~44 mM), acetate (~30 mM), and butyrate (~50 mM) concentrations (Fig. 1c). Hence, at pH 5.7, the acetate and butyrate concentrations were comparable to the wild-type titers (~31 and ~57 mM, respectively). After samples were drawn for subsequent transcriptome analyses (t=120 h), the pH shift was initiated by temporary deactivation of the pH control to induce solvent formation. The pH decreased to pH 4.5 within 9 h, and 48 h after the automatic pH regulation was re-started, steady-state solventogenic growth was attained. Only small amounts of acetone (~2 mM) and significantly lower butanol titers (~24 mM) were measured as compared to the wild-type strain (~20 and ~45 mM, respectively). In accordance with previous batch fermentation studies, alcohol production was clearly reduced, although the ABE ratio was improved in favor of butanol (Lehmann et al. 2012a). The resulting final molar BE/A ratio was 20 for the *adc* mutant, in contrast to a ratio of 3 for the wild type. Furthermore, butyrate levels dropped from ~50 to ~5 mM, whereas up to ~35 mM acetate was measured during steady-state conditions at pH 4.5 (as compared to ~14 mM in the wild-type culture).

One major rationale in order to direct the carbon flux towards butanol as the desired end product is the reduction of by-product formation and the identification and/or elimination of metabolic bottlenecks. Since the *adc*::int(180) mutant accumulated large amounts of acetate, the *pta* gene was additionally disrupted in this genetic background, yielding strain *C. acetobutylicum adc*::int(180)ΔRAM-*pta*::int(80) (Lehmann et al. 2012a). In previous batch cultivation experiments, the double knockout mutant revealed significantly reduced acetate production and a much lower glucose consumption rate as compared to the wild type. Although the metabolic flux towards butyryl-CoA was obviously increased, a drastically reduced solvent production and high butyrate concentrations were detected in the fermentation broth (Lehmann et al. 2012a). It was previously shown that in fermentations without pH control where the concentration of undissociated acids exceeded a critical threshold value, the switch from acidogenesis to solventogenesis failed to occur, a phenomenon known as "acid crash" (Kumar et al. 2013; Maddox et al. 2000; Wang et al. 2011). Therefore, we examined the behavior of the *adc*::int(180)ΔRAM-*pta*::int(80) strain in a pH-controlled chemostat cultivation experiment. Acidogenic steady-state growth at pH 5.7 was reached after 108 h with a stable OD_{600} of 4, as well as constant glucose (~52 mM), acetate (~5 mM), and butyrate (~57 mM) concentrations (Fig. 1d). Hence, the low-acetate phenotype of the double knockout mutant was confirmed, and the butyrate concentration remained the same as in the wild type

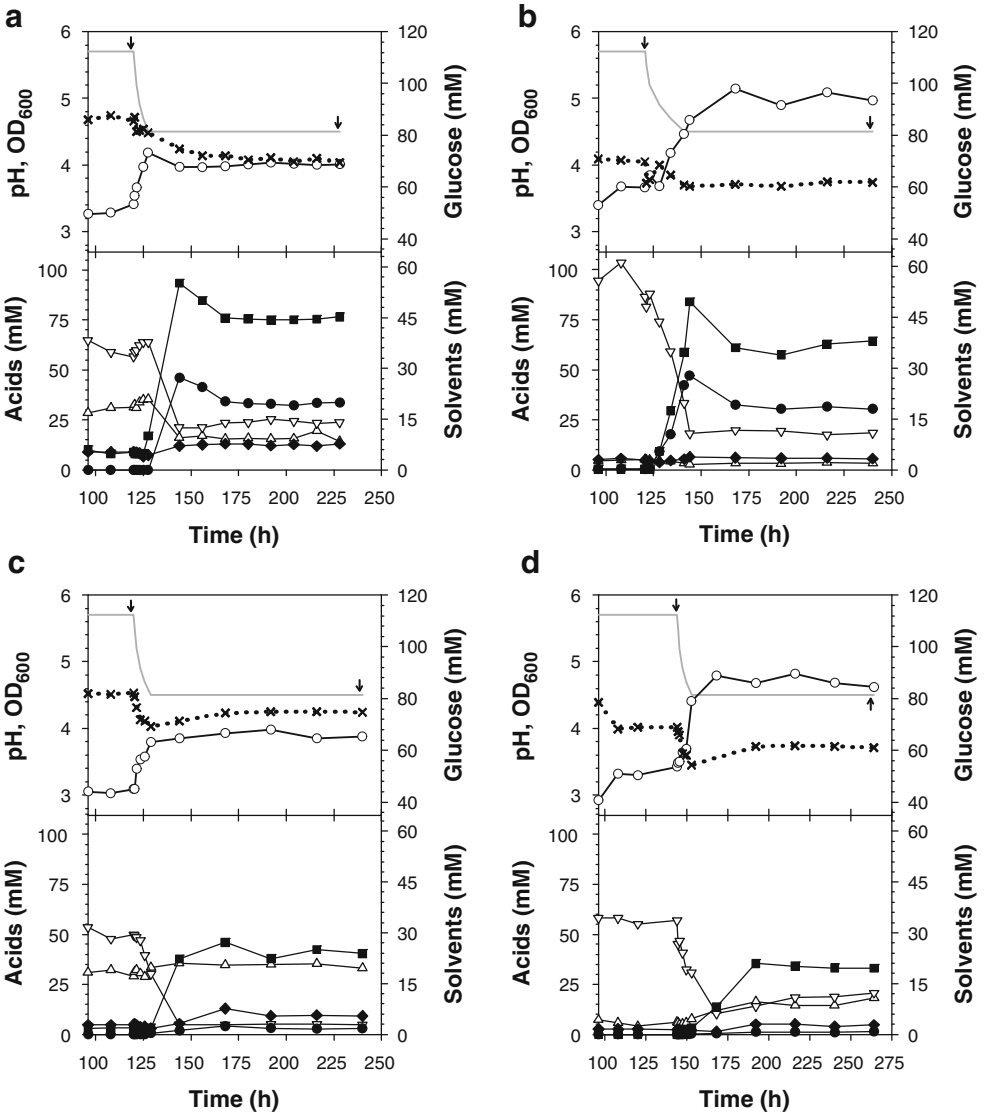

Fig. 1 Fermentation profiles of *C. acetobutylicum* ATCC 824 (**a**) and its mutants *pta*::int(80) (**b**), *adc*::int(180), (**c**) and *adc*::int(180)ΔRAM-*pta*::int(80) (**d**). The strains were cultivated anaerobically in a pH-controlled chemostat until steady-state conditions at pH 5.7 and pH 4.5 were adjusted. Samples were regularly drawn to monitor growth (*dotted black line, x*), pH (*solid gray line*), and glucose concentrations (*solid black line, open circle*). The fermentation products butyrate (*open triangle down*), acetate (*open triangle up*), ethanol (*filled diamond*), acetone (*filled circle*), and butanol (*filled square*) were measured by gas chromatography. *Arrows* indicate sampling points for transcriptome analyses

(~57 mM). After sampling for DNA microarray experiments (t=144 h), the pH control was turned off and the pH decreased through natural acidification within 8 h and 40 min to pH 4.5. The subsequent return to pH regulation resulted in solventogenic steady-state growth at pH 4.5 after 192 h of total cultivation time with a stable OD_{600} of 3.72 and a constant glucose concentration of ~86 mM, which was about 20 % higher than in the wild type (~69 mM). Furthermore, acetate concentrations were threefold higher (~15 mM) at pH 4.5 than during acidogenic growth, and butyrate levels dropped from ~57 to ~19 mM. Solvent production by the double knockout mutant reached concentrations of ~20, ~1, and ~3 mM for butanol, acetone, and ethanol, respectively. This is much lower than the wild type with ~45, ~20, and ~8 mM, respectively. Among all strains analyzed in this work, *C. acetobutylicum adc*::int(180)ΔRAM-*pta*::int(80) exhibited the lowest solvent production (Fig. 5).

Transcription analysis of central metabolic genes

Acidogenic and solventogenic cells of *C. acetobutylicum* ATCC 824 and its mutants were comprehensively compared by DNA microarray analyses to provide new insights into the cellular gene expression programs. Significance was defined by a threefold up- or downregulation, i.e., expression ratios of ≥3.0 and ≤−3.0 were considered to be significant. The interpretation of microarray data was divided into the examination of genes encoding central metabolic enzymes (Table 1), and a subset of other genes with significantly altered transcript levels (Table 2).

Regarding alcohol forming pathways of *C. acetobutylicum*, significant differences in gene expression ratios were observed for the pSOL1-encoded bifunctional aldehyde/alcohol dehydrogenase gene *adhE2* (CAP0035) in all three mutant strains as compared to the wild type (Table 1). The transcript levels of CAP0035 were highly upregulated in the *pta* mutant

(~44-fold at pH 5.7 and ~583-fold at pH 4.5) and in the *adc*/*pta* double mutant (~38-fold at pH 5.7 and ~283-fold at pH 4.5). In contrast, the *adc* mutant showed a decreased *adhE2* expression ratio of −4.19 during solventogenic growth, whereas the gene products of the *sol*-operon (CAP0162 to CAP0164) were upregulated (Table 1). During acidogenic steady-state growth of the *adc* mutant, no clear changes in the transcription patterns of *adhE2* (CAP0035), *adhE1* (CAP0162), or the subunits of the acetoacetyl-CoA:acyl-CoA-transferase (CoAT) (CAP0163 to CAP0164) were observed.

Furthermore, the L-lactate dehydrogenase encoding gene CAC0267 exhibited significantly higher expression values in the *pta* mutant and the *adc*/*pta* double mutant strains but a slightly decreased value in the *adc* mutant. The *pta* mutant revealed an expression ratio of 7.44-fold at pH 5.7 and 6.40-fold at pH 4.5. The double knockout mutant showed an upregulation of 3.08-fold at pH 5.7 and 7.20-fold during solventogenic steady-state growth at pH 4.5. Despite the increased expression levels, none of the mutant strains exhibited significant lactate concentrations during cultivation.

The butyryl-CoA synthesis (*bcs*) operon which consists of *hbd* (CAC2708), *crt* (CAC2712), *bcd* (CAC2711), and two electron transfer flavoproteins *etfA* (CAC2709) and *etfB* (CAC2710), as well as the primary thiolase gene *thlA* (CAC2873), exhibited distinctly altered transcription profiles only in the *adc*/*pta* double mutant (Table 1). The significant upregulation of these genes supports the hypothesis of an increased intracellular availability of butyryl-CoA, resulting in C_4 compounds as the main fermentation products, i.e., butyrate at pH 5.7 and butanol at pH 4.5, respectively (Fig. 1d).

Not surprisingly, analyses of acetate biosynthetic genes revealed decreased expression levels of the acetate kinase (*ack*) gene located in the bicistronic *pta*-*ack*-operon in *C. acetobutylicum* mutants with disrupted *pta* gene. However, *ack* and *pta* expression levels were not significantly altered in the *adc* mutant strain, although increased acetate concentrations

Table 1 Transcriptional profiles of central metabolic genes of the *C. acetobutylicum* mutants *pta*::int(80), *adc*::int(180), and *adc*::int(180)ΔRAM-*pta*::int(80)

ORF	Genes	Proteins	*pta*::int(80)		*adc*::int(180)		*adc*::int(180)ΔRAM-*pta*::int(80)	
			pH 5.7 (*t*=120 h)	pH 4.5 (*t*=240 h)	pH 5.7 (*t*=120 h)	pH 4.5 (*t*=240 h)	pH 5.7 (*t*=144 h)	pH 4.5 (*t*=264 h)
CAP0025	*pdc*	Pyruvate decarboxylase	1.09	−1.12	1.81	1.24	1.02	1.52
CAP0035	*adhE2*	Aldehyde/alcohol dehydrogenase (NADH)	44.11	582.62	−1.18	−4.19	37.56	283.05
CAP0078	*thlB*	Acetyl-CoA acetyltransferase	1.33	1.25	1.35	1.90	1.16	2.35
CAP0162	*adhE1*	Aldehyde/alcohol dehydrogenase (NADH)	3.09	1.05	1.43	3.50	−1.40	3.38
CAP0163	*ctfA*	Butyrate-acetoacetate CoA transferase subunit A	3.41	1.06	1.79	3.28	−1.50	3.51
CAP0164	*ctfB*	Butyrate-acetoacetate CoA transferase subunit B	2.42	1.92	1.80	4.08	1.08	2.51
CAP0165	*adc*	Acetoacetate decarboxylase	2.83	−1.16	–	–	–	–
CAC0267	*ldh*	L-lactate dehydrogenase	7.44	6.40	−1.63	−1.44	3.08	7.20
CAC1742	*pta*	Phosphotransacetylase	–	–	−1.27	−1.00	–	–
CAC1743	*ack*	Acetate kinase	−16.26	−14.52	−1.29	1.21	−1.81	−1.40
CAC2229	*pfor*	Pyruvate:ferredoxin oxidoreductase	−1.67	1.07	−1.18	1.16	1.17	2.82
CAC2708	*hbd*	3-Hydroxybutyryl-CoA dehydrogenase	1.48	3.04	−1.17	−1.63	2.70	4.37
CAC2709	*etfA*	Electron transfer flavoprotein subunit A	1.63	2.74	−1.11	−1.22	2.03	7.61
CAC2710	*etfB*	Electron transfer flavoprotein subunit B	1.80	2.10	−1.24	−1.42	1.40	4.63
CAC2711	*bcd*	Butyryl-CoA dehydrogenase	1.62	1.80	−1.05	−1.44	1.70	5.49
CAC2712	*crt*	Enoyl-CoA hydratase	1.42	2.24	−1.09	−1.84	2.00	3.88
CAC2873	*thlA*	Acetyl-CoA acetyltransferase	1.53	3.78	−1.73	−1.79	1.71	4.72
CAC3075	*buk*	Butyrate kinase	1.11	1.40	−1.01	−1.56	1.15	2.80
CAC3076	*ptb*	Phosphate butyryltransferase	1.57	1.37	1.17	−1.61	1.14	3.01
CAC3298	*bdhA*	Butanol dehydrogenase A	−1.06	−1.32	−1.33	1.06	−1.33	−1.50
CAC3299	*bdhB*	Butanol dehydrogenase B	1.19	−1.11	1.09	1.27	−1.02	−1.04

RNA samples were drawn from steady-state acidogenic and solventogenic cells, respectively, and hybridized with corresponding wild-type RNA samples. Expression ratios of ≥3.0 and ≤−3.0 were considered as significantly increased or repressed, respectively. Genes are listed in order of ORF numbers

ORF open reading frame

Table 2 Subset of genes considered as significantly increased (≥3.0) or repressed (≤−3.0) at the transcript level of the *C. acetobutylicum* mutants *pta*::int(80), *adc*::int(180), and *adc*::int(180)ΔRAM-*pta*::int(80)

ORF	Genes	Proteins	*pta*::int(80)		*adc*::int(180)		*adc*::int(180)ΔRAM-*pta*::int(80)	
			pH 5.7 (*t*=120 h)	pH 4.5 (*t*=240 h)	pH 5.7 (*t*=120 h)	pH 4.5 (*t*=240 h)	pH 5.7 (*t*=144 h)	pH 4.5 (*t*=264 h)
CAP0036		Uncharacterized, ortholog of YgaT gene of *B. subtilis*	1.21	78.77	1.66	−1.56	1.03	15.40
CAP0037		Uncharacterized, ortholog of YgaS gene of *B. subtilis*	1.08	113.05	1.33	−1.64	1.21	18.49
CAP0066		ptna mannose-specific phosphotransferase system component IIAB	n.d.	n.d.	385.57	n.d.	1,599.60	n.d.
CAP0067		manY/levF mannose/fructose-specific phosphotransferase system component IIC	382.67	600.72	502.11	128.93	1,038.56	n.d.
CAP0068		ptnd mannose-specific phosphotransferase system component IID	173.94	582.21	360.98	n.d.	n.d.	n.d.
CAP0168	*amyA*	Alpha-amylase	5.19	3.07	1.40	−1.14	2.39	1.81
CAC0102		*O*-acetylhomoserine sulfhydrylase	−6.02	5.46	4.43	103.59	−2.59	1.30
CAC0103	*cysC*	Adenylylsulfate kinase	−8.15	10.84	4.73	157.42	−2.65	n.d.
CAC0104		Adenylylsulfate reductase	−9.88	n.d.	4.65	146.36	−2.38	n.d.
CAC0105	*fer*	Ferredoxin	−8.14	6.78	3.77	98.17	−2.13	1.68
CAC0106		ABC-type probable sulfate transporter, periplasmic binding protein	−5.57	3.11	3.47	27.64	−1.97	1.90
CAC0107		ABC-type sulfate transporter, ATPase component	−7.71	12.16	2.48	110.44	−1.52	1.52
CAC0108		ABC-type probable sulfate transporter, permease protein	−7.90	6.65	2.96	60.58	−1.60	n.d.
CAC0109	*cysD*	Sulfate adenylyltransferase subunit 2	−7.84	11.61	1.89	116.37	−1.26	1.57
CAC0110	*cysN*	GTPase, sulfate adenylate transferase subunit 1	−3.89	n.d.	1.96	44.42	1.18	1.35
CAC0118	*cheA*	Chemotaxis protein CheA	−1.46	1.24	−3.24	−1.13	−3.08	−3.04
CAC0120		Membrane-associated methyl-accepting chemotaxis protein	−1.45	2.13	−3.59	1.22	n.d.	n.d.
CAC0304	*motA*	Chemotaxis protein MotA	−29.82	−2.76	−33.94	−4.85	−21.33	−1.63
CAC0305	*motB*	Chemotaxis protein MotB	−25.60	−3.33	−24.77	−5.62	−18.18	−3.06
CAC0390		Cystathionine gamma-synthase	1.06	1.26	1.92	18.77	n.d.	n.d.
CAC0391		Cystathionine beta-lyase	1.08	1.19	1.76	13.24	n.d.	n.d.
CAC0443		Methyl-accepting chemotaxis protein	−20.00	n.d.	n.d.	n.d.	−10.55	n.d.
CAC0929		SAM-dependent methyltransferase	−1.32	−1.52	3.93	9.84	1.11	1.51
CAC0930	*metB*	Cystathionine gamma-synthase	−1.54	−1.49	5.23	14.55	1.94	1.34
CAC0931		Cysteine synthase	−1.81	1.11	5.58	15.91	3.59	1.06
CAC0980	*pflB*	Pyruvate-formate-lyase	2.96	1.07	1.43	−1.12	1.44	1.20
CAC0981	*pflA*	Pyruvate-formate-lyase-activating enzyme	4.17	−1.03	1.75	−1.15	1.89	−1.22
CAC1233	*cheV*	Chemotaxis protein CheV	−14.49	n.d.	n.d.	n.d.	n.d.	n.d.
CAC1548	*trxB*	Thioredoxin reductase	−1.96	−1.40	−4.20	1.87	−7.78	2.21
CAC1571		Glutathione peroxidase	−4.80	−1.41	−4.04	1.17	−3.64	1.32
CAC1600		Methyl-accepting chemotaxis-like protein	−8.10	−3.74	−13.98	−3.53	−11.07	−3.09
CAC1601		Methyl-accepting chemotaxis-like protein	−8.23	−4.21	−11.73	−3.85	−9.89	−4.56
CAC1634		Flagellin	−107.90	n.d.	−157.50	n.d.	−59.06	−32.34
CAC1825	*metB*	Homoserine *O*-succinyltransferase	−1.54	1.12	1.42	9.99	−1.18	1.33
CAC2167		Flagellin family protein	−5.99	−2.54	−5.75	−1.53	−5.97	−1.64
CAC2203	*hag*	Hook-associated protein, flagellin family	−62.47	−12.80	−58.13	−10.11	−34.91	−8.19
CAC2204		Hypothetical protein	−4.28	−1.68	−5.84	−1.85	−5.70	−2.22
CAC2205	*fliD*	Lagellar hook-associated protein FliD	−7.60	−2.99	−6.68	−1.82	−8.24	−2.30
CAC2206	*fliS*	Flagellar protein FliS	−7.26	−3.39	−6.95	−2.48	−8.23	−3.62
CAC2207		Hypothetical protein	−6.01	−2.01	−6.55	−1.54	−7.74	−1.61
CAC2208	*flaG*	Flagellin, flagellar protein FlaG	−6.10	−2.63	−7.73	−2.20	−8.07	−2.38
CAC2209	*csrA*	Carbon storage regulator, csrA	−6.69	−2.95	−8.19	−2.19	−9.16	−2.87

Table 2 (continued)

ORF	Genes	Proteins	*pta*::int(80)		*adc*::int(180)		*adc*::int(180)ΔRAM-*pta*::int(80)	
			pH 5.7 (*t*=120 h)	pH 4.5 (*t*=240 h)	pH 5.7 (*t*=120 h)	pH 4.5 (*t*=240 h)	pH 5.7 (*t*=144 h)	pH 4.5 (*t*=264 h)
CAC2210	*fliW*	Flagellar assembly protein FliW	−9.05	−2.30	−10.06	−2.29	−11.63	−2.87
CAC2211	*flgL*	Flagellin, flagellar hook-associated protein 3 FlgL	−9.66	−2.81	−11.88	−2.22	−9.98	−1.97
CAC2212	*flgK*	Flagellar hook-associated protein FlgK	−8.84	−2.93	−9.72	−2.63	−9.91	−3.32
CAC2213		Hypothetical protein	−7.71	−3.28	−8.46	−2.41	−9.28	−3.70
CAC2214	*flgM*	Flagellin synthesis regulator FlgM	−7.50	−2.47	−9.05	−2.31	−8.55	−3.15
CAC2235	*cysK*	Cysteine synthase/cystathionine beta-synthase	−2.60	1.94	2.19	14.27	−1.71	−1.93
CAC2783	*cysD*	*O*-acetylhomoserine sulfhydrylase	−1.25	1.85	1.58	11.99	−1.49	−1.20
CAC2963	*lacG*	6-Phospho-beta-D-galactosidase	24.33	52.30	31.34	19.78	50.71	21.84
CAC2964	*lacE*	PTS system lactose-specific enzyme IIBC	26.28	49.57	34.97	24.24	52.58	18.47
CAC2965	*lacF*	PTS system lactose-specific enzyme IIA	37.88	96.30	47.12	n.d.	100.04	n.d.
CAC2966	*lacR*	Lactose phosphotransferase system repressor lacR	n.d.	n.d.	69.09	n.d.	n.d.	n.d.
CAC3169	*ilvB*	Acetolactate synthase large subunit	3.62	1.17	1.08	1.37	−1.06	−3.31
CAC3170	*ilvD*	Dihydroxy-acid dehydratase	3.20	1.74	1.08	1.49	−1.13	−3.10
CAC3171	*leuB*	Isopropylmalate dehydrogenase	3.29	1.31	1.18	1.18	1.12	−4.45
CAC3172	*leuD*	3-Isopropylmalate dehydratase, small subunit	3.14	1.18	1.24	1.14	1.01	−4.63
CAC3173	*leuC*	3-Isopropylmalate dehydratase	3.74	1.02	1.37	1.12	−1.10	−5.50
CAC3174	*leuA*	2-Isopropylmalate synthase	3.77	1.15	1.55	1.26	1.04	−4.01
CAC3352		Methyl-accepting chemotaxis protein	−2.83	−3.49	−4.49	−2.24	−4.52	−2.01
CAC3510		Methyl-accepting chemotaxis protein	−2.24	−1.24	−4.11	−1.37	−3.17	1.51

RNA samples were drawn from steady-state acidogenic and solventogenic cells, respectively, and hybridized with corresponding wild-type RNA samples. Genes are listed in order of ORF numbers

n.d. no ratio was calculated due to used filter criteria of the microarray, *ORF* open reading frame

were detected, particularly in the solventogenic phase. Similarly, expression of the butyrate kinase (*buk*) and the *ptb* genes did not show significant upregulation, although the *pta* and *adc*/*pta* double mutants exhibited high butyrate concentrations in the culture medium.

Global transcription analysis

Assessment of the global transcriptional changes in the three mutant strains is summarized in Fig. 2, where significantly upregulated and downregulated genes are compared in Venn diagrams during both acidogenic (Fig. 2a) and solventogenic growth (Fig. 2b). The *pta* mutant exhibited a significant downregulation (−8.14-fold) during acidogenic growth at pH 5.7 (Table 2) of genes related to sulfate assimilation, i.e., the genes for sulfate transport (CAC0106 to CAC0108), and conversion of intracellular sulfate and serine to cysteine (CAC0103, CAC0104, CAC0109, CAC0110) including CAC105 coding for one of five putative ferredoxins and of CAC0102 involved in the synthesis of methionine (Nölling et al. 2001). During solventogenic steady-state growth at pH 4.5 of the *pta* mutant strain, the genes for sulfate assimilation genes were significantly induced up to ~157-fold. The transcription analysis of the *adc* mutant revealed elevated transcript levels of genes required for the conversion of sulfide to cysteine (CAC0931, CAC2235), cysteine to homocysteine (CAC0390 and CAC0391), homoserine to cystathione (CAC1825, CAC0930), and *O*-succinyl-L-homoserine to homocysteine (CAC0102 and CAC2783) (Table 2). Interestingly, the transcription of genes involved in the synthesis of organic sulfur metabolites was not significantly changed in the *adc*/*pta* double mutant, neither during acidogenic nor during solventogenic steady-state growth.

A cluster of genes (CAC3169 to CAC3176) encoding some of the enzymes for branched chain amino acid synthesis exhibited elevated transcript patterns in the *pta* mutant strain during acidogenic growth at pH 5.7, which was in accordance with a previous study where these genes were upregulated as a response to butyrate stress (Alsaker et al. 2010).

In all three mutant strains, the pSOL1-encoded fructose/mannose phosphotransferase system (PTS) (CAP0066 to CAP0068) and the chromosomal lactose phosphotransferase system (CAC2963 to CAC2965) showed strongly upregulated transcript levels throughout both acidogenic and solventogenic steady-state growth. In addition, genes related to flagellin proteins and chemotaxis were significantly

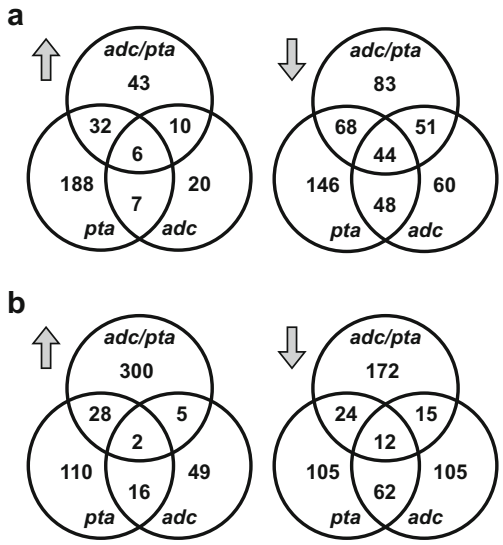

Fig. 2 Venn diagrams of the number of significantly induced or repressed genes of *C. acetobutylicum* mutants during acidogenesis (**a**) and solventogenesis (**b**). Significant upregulation (i.e., ≥3.0) is shown on the *left* (*arrow up*) and significant downregulation (i.e., ≤-3.0) is illustrated in the *right panels* (*arrow down*). *pta*, *C. acetobutylicum pta*::int(80); *adc*, *C. acetobutylicum adc*::int(180); *adc/pta*, *C. acetobutylicum adc*::int(180)ΔRAM-*pta*::int(80)

repressed in the three knockout mutants during acidogenic growth (Table 2).

The ORFs for two proteins CAP0036 and CAP0037, annotated as uncharacterized gene products with unknown functions (Nölling et al. 2001), constitute a bicistronic transcription unit with a length of ~1.4 kb and were shown to be highly upregulated during acidogenic growth but strongly repressed during solventogenic steady-state growth in continuous cultures of *C. acetobutylicum* (Grimmler et al. 2011; Janssen et al. 2010). Again, the transcription pattern of the *adc* mutant differed from that of the *pta* and *adc*/*pta* mutants. Whereas CAP0036 and CAP0037 were slightly downregulated in the *adc*-negative strain, both other mutants exhibited highly increased transcript levels during solventogenic steady-state growth as compared to the parental wild type (Table 2).

Disruption of the butyrate pathway

Continuous cultures and product patterns

It was previously shown that no butyrate was detected in cultures of the phosphotransbutyrylase-negative *ptb*::int(87) mutant, indicating that the acetate-forming phosphotransacetylase cannot substitute the phosphotransbutyrylase reaction (Lehmann et al. 2012b). In this study, we used continuous cultures to study the metabolic and transcriptional changes of the *ptb* mutant in more detail. The cells reached acidogenic steady-state growth at pH 5.7 after 108 h (Fig. 3a), showing an acetate concentration of ~54 mM, which was 43 % higher than in the wild type (~31 mM). In accordance with previous batch cultivation experiments (Lehmann et al. 2012b), butyrate was never detectable in the culture supernatant samples. Surprisingly, up to 30 mM of butanol was detected during acidogenic growth at pH 5.7, and measurements of these significant amounts of butanol were repeated several times to ensure reproducibility. One hundred twenty hours after starting the continuous culture, samples were taken for transcription analysis. Subsequently, the pH regulation was discontinued and the pH decreased in 13.5 h from 5.7 to pH 4.5. During the pH shift, the glucose concentration in the medium supernatant increased from 70.16 to 84.15 mM, while the optical density decreased from 4.0 to 3.62. When the culture reached solventogenic steady-state growth at pH 4.5, the glucose concentration in the supernatant decreased to 78.77 mM, and the OD remained constant at an OD_{600} of 3.7. After the optical density and the glucose concentration in the medium had remained stable for at least three volume changes, cells were collected for subsequent DNA microarray experiments. Solvent production of the *ptb* mutant reached concentrations of ~44 mM butanol and ~23 mM acetone, which was comparable to the wild type (~45 and ~20 mM, respectively). In batch fermentations where the pH was kept above 5.0, the product pattern of the *ptb* mutant revealed a high ethanol titer of 12.1 g/l (Lehmann et al. 2012b), while in contrast, ethanol production was only negligibly increased in our continuous cultures (Fig. 3a). Similarly, batch cultivation experiments without pH control in MS-MES without acetate resulted in high lactate levels of >40 mM (Lehmann et al. 2012b), whereas lactate concentrations in continuous cultures of the *ptb* mutant were always <1 mM.

Continuous cultivation in the presence of butyrate

Since the *ptb* mutant provided a suitable experimental basis to analyze butyrate uptake due to its butyrate-negative phenotype, butyrate feeding experiments were conducted without interference of butyrate synthesis by the cells. To this end, we conducted continuous cultivations of the *ptb* mutant in a medium that contained 20 mM butyrate.

Metabolite analyses revealed ~68 mM acetate during acidogenic growth at pH 5.7, which was about 54 % more than in the wild type (~31 mM), as well as ~5 mM lactate. Again, high concentrations of butanol (~34 mM) were detected under acidogenic conditions. One hundred seventy hours after starting the continuous cultivation, the pH control was switched off in order to induce the shift to solventogenic growth. During the course of the pH shift, the glucose concentration in the medium supernatant increased from ~69 to ~95 mM, suggesting that the glucose consumption by the cells was considerably decreased. At the same time, the optical

density decreased to a value of 2.61, followed by a significant drop to 1.45 within the subsequent 16 h (t=192 h). Several hours later (t=240 h), the culture "recovered" and reached a balanced solventogenic steady-state with an OD_{600} of ~3.8. Thus, though the pH decreased to 4.5 in less than 6 h in the butyrate feeding experiment, the *ptb* mutant required an extended time period to reach stable steady-state solventogenic growth at pH 4.5 as compared to a continuous culture without butyrate (Fig. 3). During solventogenic growth, butyrate concentrations were approximately half of the supplied 20 mM butyrate (Fig. 3b). Hence, the *ptb* mutant clearly assimilated the externally provided butyrate (Fig. 3b), which was in agreement with the butyrate feeding experiments using batch cultures (Lehmann et al. 2012b). The decrease of the acetate concentration from ~68 to ~27 mM indicates acetate re-assimilation, while lactate was no longer detectable. In comparison to the wild type and the *ptb* mutant without butyrate feeding, the acetone and butanol titers were roughly halved, whereas the ethanol concentrations were slightly increased to ~17 mM. For transcription analysis, cells were collected after 170 h (pH 5.7), at the end of the pH shift (pH 4.5), and after 264 h (pH 4.5) as indicated by the arrows in Fig. 3b.

Transcription analysis of central metabolic genes

Transcription analyses of the *ptb* mutant in continuous cultures were performed using steady-state samples of acidogenic and solventogenic cells with or without butyrate feeding. In addition to acidogenesis and solventogenesis, RNA samples were also collected during the "recovery" phase after the pH shift in order to investigate the transcription patterns of the transition phase.

The transcriptional profiles of genes related to the central fermentative metabolism in *C. acetobutylicum ptb*::int(87) in the presence and absence of butyrate are summarized in Fig. 4. During solventogenic steady-state growth of the *ptb* mutant, the pSOL1-encoded *adhE2* (CAP0035) was found to be highly upregulated (~33-fold) when compared to the parental wild type, whereas the transcription was increased ~2.4-fold as compared to the wild type during acidogenic growth. Continuous cultivation of the *ptb* mutant in the presence of 20 mM butyrate in the feed medium led to significantly increased transcription of the *adhE2* gene during acidogenic growth (7.72-fold), at the end of the pH shift (5.88-fold), as well as during solventogenic growth at pH 4.5 (87.20-fold) (Table 3).

In the absence of external butyrate supplementation, transcription of the *sol*-operon harboring the alcohol/aldehyde dehydrogenase gene *adhE1* (CAP0162) as well as the *ctfA* and *ctfB* genes (CAP0163, CAP0164) for the acid CoA transferase was not significantly altered in the *ptb* mutant strain. In the presence of butyrate, the *ptb* mutant revealed a decreased transcription level of the *sol*-locus during acidogenic growth at pH 5.7 but unchanged rates after the pH shift. Interestingly, the acetoacetate decarboxylase gene *adc* (CAP0165) was clearly downregulated in comparison to the wild type (−2.76- to −4.91-fold) when butyrate was added to the medium (Table 3).

In a previous study, *C. acetobutylicum ptb*::int(87) produced high amounts of lactate during batch cultivation in mineral salts medium without pH control (Lehmann et al. 2012b). In our continuous culture study, in contrast, the *ptb* mutant strain produced only small amounts of lactate (<1 mM), and the transcription levels of the L-lactate dehydrogenase gene CAC0267 were not significantly different during acidogenic versus solventogenic growth. However, in the presence of butyrate, the *ptb* mutant excreted 5–7 mM lactate at pH 5.7 and during the pH shift, which was washed out during solventogenic growth. Accordingly, transcription of CAC0267 was upregulated ~11- to ~17-fold in the course of the fermentation (Table 3).

Throughout continuous cultivation with and without butyrate addition, the *ptb* mutant exhibited significant upregulation of some genes coding for enzymes involved in the conversion of acetyl-CoA to butyryl-CoA, i.e., *thlA* (CAC2873), *hbd* (CAC2708), *crt* (CAC2712), *bcd* (CAC2711), *etfA* (CAC2709), and *etfB* (CAC2709). As expected, expression of the butyrate kinase encoding *buk* gene (CAC3075) was drastically reduced, indicating a polar effect on its transcription caused by the intron insertion into the *ptb* gene.

Global transcription analysis

During acidogenic steady-state growth of the *ptb* mutant in the presence of 20 mM of butyrate, transcription of the genes CAC0102 to CAC0108 representing the large sulfur metabolism cluster (CAC0102 to CAC0110) was significant upregulated (Table 4). At the end of the pH shift at pH 4.5 (t= 175.67 h), all genes of this cluster (CAC0102-CAC0110) were induced up to ~15-fold, and during solventogenic steady-state conditions (t=264 h), the expression level of these genes was close to the value defined as significant downregulation when compared to the wild type. Furthermore, genes for the conversion of *O*-succinyl-L-homoserine to homocysteine (CAC2783) and cysteine to homocysteine (CAC0390 and CAC0391) were significantly upregulated during acidogenesis and at the end of the pH shift. For the latter two genes, significantly decreased transcript values were determined during solventogenic steady-state growth of the mutant. Without butyrate in the supplying medium, the *ptb* mutant strain revealed clearly induced expression of the genes CAC0102 to CAC0110 and CAC0390 to CAC0391 during solventogenic steady-state growth at pH 4.5 (Table 4).

As noticed for the *pta*-, *adc*-, and *adc*/*pta*-negative mutants, motility and chemotaxis encoding genes were downregulated

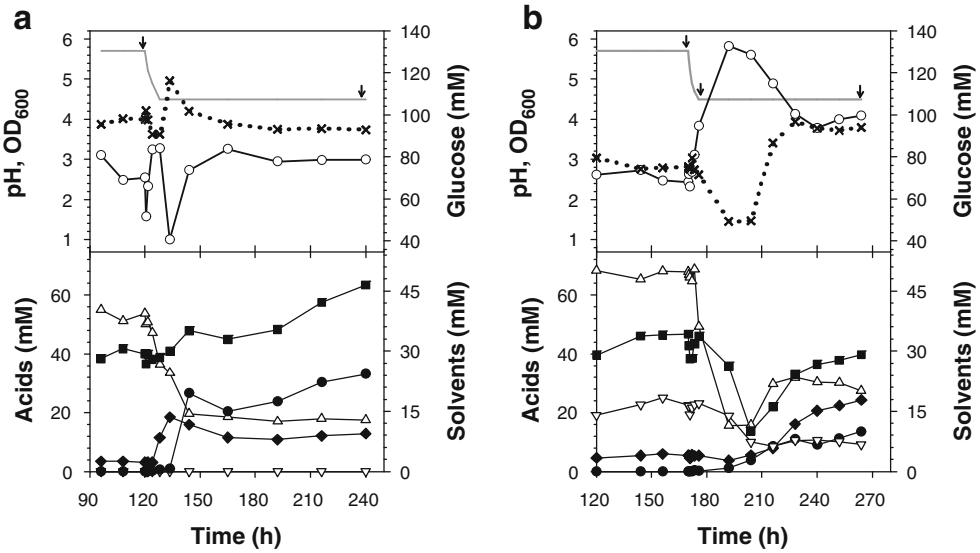

Fig. 3 Fermentation profiles of *C. acetobutylicum ptb*::int(87) in the absence (**a**) and presence of 20 mM butyrate in the supplying medium (**b**). Cultivation conditions, lines, and symbols are the same as for Fig. 1

in the *ptb* mutant strain, irrespective whether butyrate was added or not. With respect to the peculiar expression patterns of the uncharacterized genes CAP0036 and CAP0037 described above, both genes showed a drastic repression in the *ptb* mutant, independent of the cultivation conditions. Also, similar to the expression profiles of the other three strains, the *ptb* mutant exhibited a strongly increased transcription of the pSOL1-encoded fructose/mannose PTS genes (CAP0066 to CAP0068) and the chromosomal lactose PTS genes (CAC2963 to CAC2966). Adding butyrate to the feed medium resulted in a further upregulation of these genes when compared to the wild type. However, during the pH shift and subsequent "recovery," the expression ratio of those genes first decreased (to 1.23- to 1.36-fold) prior to a sharp increase of 21.63- to 34.72-fold during steady-state conditions at pH 4.5 (Table 4).

Finally, two other gene clusters where differently regulated in the *ptb* mutant than in the *pta*-, *adc*-, and *adc*/*pta*-negative strains. In one case, several *nif* genes (CAC0256 to CAC0261) were significantly induced in the *ptb* mutant. In the other case, the *pflA* and *pflB* genes, coding for a putative formate lyase (CAC0980) and its activating enzyme (CAC0981), exhibited increased expression ratios, particularly during the pH shift in the butyrate feeding experiment (Table 4).

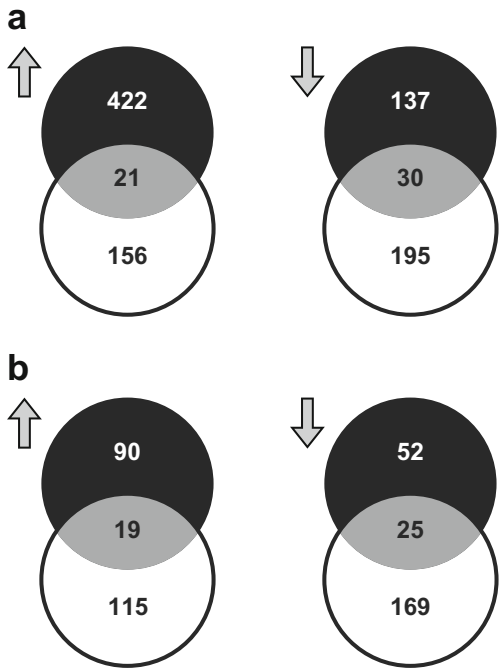

Fig. 4 Venn diagrams of the number of significantly induced or repressed genes of *C. acetobutylicum ptb*::int(87) mutant in the absence (*black*) and presence of 20 mM butyrate (*white*) during acidogenesis (**a**) and solventogenesis (**b**). Significant upregulation (i.e., ≥3.0) is shown on the *left* (*arrow up*) and significant downregulation (i.e., ≤−3.0) is illustrated in the *right panels* (*arrow down*)

Discussion

Continuous cultivation allows the analysis of microbial physiology in steady-state growth with constant environmental parameters. Solventogenic clostridia show very variable fermentation profiles in batch cultures depending on many details of the actual cultivation due to the consumption of substrates and the accumulation of various acidic fermentation products that are later taken up again, associated with constantly changing growth rate and pH, superimposed with cell differentiation processes such as the accumulation of storage products and endospore formation. Chemostat cultures can bypass these complex physiological and morphological changes, because the cells can be kept in defined steady states and are therefore particularly suitable for "omics" studies (Grimmler et al. 2011; Janssen et al. 2010). In this study, recently constructed

Table 3 Transcriptional profiles of central metabolic genes of *C. acetobutylicum ptb*::int(87) in the absence and presence of 20 mM butyrate in the supplying medium

ORF	Genes	Proteins	*ptb*::int(87)		*ptb*::int(87) + 20 mM butyrate		
			pH 5.7 (t=120 h)	pH 4.5 (t=240 h)	pH 5.7 (t=170 h)	pH 4.5 (t=175.67 h)	pH 4.5 (t=264 h)
CAP0025	*pdc*	Pyruvate decarboxylase	−5.45	−1.72	−6.84	−6.73	−1.55
CAP0035	*adhE2*	Aldehyde/alcohol dehydrogenase (NADH)	2.41	32.57	7.72	5.88	87.20
CAP0078	*thlB*	Acetyl-CoA acetyltransferase	−1.27	−1.02	1.54	2.88	−1.10
CAP0162	*adhE1*	Aldehyde/alcohol dehydrogenase (NADH)	−1.33	−1.15	−1.90	1.57	1.44
CAP0163	*ctfA*	Butyrate-acetoacetate CoA transferase subunit A	−1.45	−1.43	−3.38	2.22	1.22
CAP0164	*ctfB*	Butyrate-acetoacetate CoA transferase subunit B	−1.78	−1.05	−4.36	−1.02	1.10
CAP0165	*adc*	Acetoacetate decarboxylase	1.29	−1.81	−3.91	−4.91	−2.76
CAC0267	*ldh*	L-lactate dehydrogenase	2.10	2.05	12.05	17.26	11.36
CAC1742	*pta*	Phosphotransacetylase	1.31	1.66	2.23	1.41	1.34
CAC1743	*ack*	Acetate kinase	1.15	1.72	2.36	1.15	1.19
CAC2229	*pfor*	Pyruvate:ferredoxin oxidoreductase	−1.33	1.21	2.23	−1.04	−1.09
CAC2708	*hbd*	3-Hydroxybutyryl-CoA dehydrogenase	1.28	3.14	2.22	1.40	2.33
CAC2709	*etfA*	Electron transfer flavoprotein subunit A	1.53	3.09	3.37	2.12	2.78
CAC2710	*etfB*	Electron transfer flavoprotein subunit B	1.38	2.92	2.63	2.21	2.01
CAC2711	*bcd*	Butyryl-CoA dehydrogenase	1.67	3.09	3.09	2.41	2.93
CAC2712	*crt*	Enoyl-CoA hydratase	1.59	3.57	2.82	2.64	3.03
CAC2873	*thlA*	Acetyl-CoA acetyltransferase	1.69	3.12	2.41	−1.74	2.91
CAC3075	*buk*	Butyrate kinase	−34.86	−32.93	−27.28	−33.55	−22.32
CAC3076	*ptb*	Phosphate butyryltransferase	–	–	–	–	–
CAC3298	*bdhA*	Butanol dehydrogenase A	1.36	−1.26	−1.09	−2.05	−2.80
CAC3299	*bdhB*	Butanol dehydrogenase B	−1.60	−1.15	−1.60	−1.47	−2.03

RNA samples were drawn from steady-state acidogenic and solventogenic cells, respectively, as well as from cells during the late pH shift of the butyrate feeding experiment. The samples used for DNA microarrays were hybridized with corresponding wild-type RNA samples. Expression ratios of ≥3.0 and ≤−3.0 were considered as significantly increased or repressed, respectively. Genes are listed in order of ORF numbers

ORF open reading frame

C. acetobutylicum mutants with disrupted acid and acetone biosynthetic pathways were characterized in continuous cultivation experiments and by comparative transcriptome analyses.

It was recently reported that the inactivation of the *ack* gene, which encodes the enzyme catalyzing the last step in acetate production, led to a reduced but not completely abolished acetate production (Cooksley et al. 2012; Kuit et al. 2012). It has also been shown that the *pta*-negative mutant *C. acetobutylicum* PJC4PTA, generated by integration of a plasmid via single crossover, revealed decreased amounts of acetate, while the butyrate formation was significantly higher than in the wild type (Green et al. 1996). In a subsequent study, data from batch cultures in static flasks showed that strain PJC4PTA produced increased amounts of butanol and diminished acetate levels, while butyrate formation was unaffected under these conditions (Zhao et al. 2005). A higher butanol production and decreased acetate concentrations were also observed for the *pta* knockout strain EKW generated by the group of Jang et al. (2012b). However, in this mutant, butyrate formation was reduced as well. Employing ClosTron mutagenesis, recently, a *pta*-negative *pta*::int(80) mutant was constructed which exhibited a similar product pattern as the wild type in batch cultures (Lehmann et al. 2012a). However, cultivation of *C. acetobutylicum pta*::int(80) in a phosphate-limited chemostat revealed reliable data on the phenotype of a *pta* mutant: whereas acetate production was clearly decreased, the butyrate level during acidogenesis was much higher than with the wild type (Fig. 5). This resembles the phenotype of strain PJC4PTA as described by Green et al. (1996). On the other hand, during steady-state solventogenic growth, we observed slightly lower alcohol titers, not an improved butanol production as described by Zhao et al. (2005).

In addition to acetate, *C. acetobutylicum* forms significant amounts of butyrate during exponential growth, which is re-assimilated after the transition to stationary growth (Lee et al. 2008). Hence, the butyrate biosynthetic pathway was also targeted by metabolic engineering attempts in order to reduce by-product formation for an improved butanol titer. Similar to *C. acetobutylicum* PJC4PTA, a butyrate kinase- (Buk) knock-out mutant was generated via single crossover integration of a

Table 4 Subset of genes considered as significantly increased (≥3.0) or repressed (≤−3.0) at the transcript level of *C. acetobutylicum ptb*::int(87) in the absence and presence of 20 mM butyrate in the supplying medium

ORF	Genes	Proteins	*ptb*::int(87)		*ptb*::int(87) + 20 mM butyrate		
			pH 5.7 (t=120 h)	pH 4.5 (t=240 h)	pH 5.7 (t=170 h)	pH 4.5 (t=175.67 h)	pH 4.5 (t=264 h)
CAP0036		Uncharacterized, ortholog of YgaT gene of *B. subtilis*	−251.95	−5.21	−131.46	−295.77	−53.63
CAP0037		Uncharacterized, ortholog of YgaS gene of *B. subtilis*	−246.79	−4.35	−111.19	−271.72	−42.86
CAP0066		ptna mannose-specific phosphotransferase system component IIAB	88.85	n.d.	56.20	n.d.	190.35
CAP0067		manY/levF mannose/fructose-specific phosphotransferase system component IIC	132.24	126.91	33.61	n.d.	151.77
CAP0068		ptnd mannose-specific phosphotransferase system component IID	63.84	n.d.	30.49	n.d.	50.07
CAP0079	*thlr*	HTH transcriptional regulator TetR/AcrR family	−1.01	1.17	1.07	3.64	1.07
CAC0102		*O*-acetylhomoserine sulfhydrylase	1.88	17.67	8.39	13.20	−1.29
CAC0103	*cysC*	Adenylylsulfate kinase	2.04	44.01	13.55	13.07	−1.21
CAC0104		Adenylylsulfate reductase	2.37	49.54	14.62	12.63	−1.13
CAC0105	*fer*	Ferredoxin	1.92	26.80	5.20	12.05	−1.14
CAC0106		ABC-type probable sulfate transporter, periplasmic binding protein	1.81	6.21	3.68	11.54	1.04
CAC0107		ABC-type sulfate transporter, ATPase component	1.85	62.96	3.84	5.62	1.37
CAC0108		ABC-type probable sulfate transporter, permease protein	n.d.	n.d.	3.69	4.94	1.46
CAC0109	*cysD*	Sulfate adenylyltransferase subunit 2	1.56	74.92	1.82	6.42	1.49
CAC0110	*cysN*	GTPase, sulfate adenylate transferase subunit 1	1.93	34.72	−1.20	6.15	1.37
CAC0256	*nifD*	Nitrogenase molybdenum-iron protein, alpha chain (nitrogenase component I) gene nifD	49.41	4.87	14.50	28.91	4.52
CAC0257	*nifK*	Nitrogenase molybdenum-iron protein, beta chain, gene nifK	9.86	2.57	10.79	4.05	3.76
CAC0258	*nifE*	Nitrogenase molybdenum cofactor biosynthesis protein NifE	38.18	5.95	21.54	15.86	8.19
CAC0259		Multifunctional nitrogenase iron-molybdenum cofactor biosynthesis protein NifN/nitrogenase molybdenum-iron protein subunit beta NifK/nitrogenase iron-molybdenum cofactor biosynthesis protein NifB	37.11	7.41	27.28	17.01	8.28
CAC0260	*nifV*	Homocitrate synthase, omega subunit nifV (nivO)	27.21	7.48	19.04	11.52	8.29
CAC0261	*nifV*	Homocitrate synthase subunit alpha NifV	15.13	4.07	9.95	3.07	3.21
CAC0304	*motA*	Chemotaxis protein MotA	−3.76	−1.99	1.13	−5.74	−3.19
CAC0305	*motB*	Chemotaxis protein MotB	−3.77	−2.50	−1.17	−3.25	−3.12
CAC0390		Cystathionine gamma-synthase	1.27	6.03	4.71	8.72	−4.02
CAC0391		Cystathionine beta-lyase	1.73	6.64	5.45	3.51	−2.59
CAC0443		Methyl-accepting chemotaxis protein	−10.17	n.d.	−3.20	n.d.	n.d.
CAC0741		Methyl-accepting chemotaxis protein	−3.18	n.d.	n.d.	n.d.	n.d.
CAC0980	*pflB*	Pyruvate-formate-lyase	1.76	2.10	4.76	18.54	2.88
CAC0981	*pflA*	Pyruvate-formate-lyase-activating enzyme	2.58	2.56	4.32	21.02	2.75
CAC1233	*cheV*	Chemotaxis protein CheV	−3.79	−2.69	−1.48	n.d.	−4.28
CAC1547	*trxA*	Thioredoxin	−2.91	−1.30	1.48	1.83	−3.57
CAC1548	*trxB*	Thioredoxin reductase	−4.76	−2.44	1.99	2.12	−3.48
CAC1549	*bsaA*	Glutathione peroxidase	−2.10	−2.48	−2.47	1.73	−4.58
CAC1570	*bsaA*	Glutathione peroxidase	−2.62	−2.30	2.05	−1.19	−3.48
CAC1634		Flagellin	−3.49	−2.66	−1.31	−9.60	−4.93
CAC2154	*flgE*	Flagellar hook protein FlgE	−3.08	−1.09	−1.03	−4.08	−1.74
CAC2156	*flgD*	Lagellar hook assembly protein FlgD	−3.57	1.11	−1.19	−3.14	−1.84
CAC2203	*hag*	Hook-associated protein, flagellin family	−5.12	−2.45	−1.43	−6.45	−7.43
CAC2211	*flgL*	Flagellin, flagellar hook-associated protein 3 FlgL	−3.04	−2.22	1.01	−3.85	−3.84

Table 4 (continued)

ORF	Genes	Proteins	*ptb*::int(87)		*ptb*::int(87) + 20 mM butyrate		
			pH 5.7 (*t*=120 h)	pH 4.5 (*t*=240 h)	pH 5.7 (*t*=170 h)	pH 4.5 (*t*=175.67 h)	pH 4.5 (*t*=264 h)
CAC2212	*flgK*	Flagellar hook-associated protein FlgK	−3.59	−2.52	−1.52	−2.65	−4.48
CAC2214	*flgM*	Flagellin synthesis regulator FlgM	−3.50	−1.99	−1.29	−2.91	−4.55
CAC2215	*fliY*	Flagellar motor switch protein	−25.45	−12.33	−25.42	−14.22	−12.33
CAC2216	*fliM*	Flagellar switch protein FliM	−9.02	−14.27	−33.95	−15.10	−12.98
CAC2217	*cheW*	Chemotaxis signal transduction protein CheW	−25.23	−16.12	−40.57	−25.54	−18.55
CAC2218	*cheY*	Chemotaxis signal receiving protein CheY	−27.18	−17.09	−37.21	−27.86	−18.00
CAC2219	*cheC*	Chemotaxis protein CheC	−25.07	−13.08	−26.37	−18.57	−14.62
CAC2221	*cheR*	Chemotaxis protein CheR	−1.81	−2.13	−3.26	−6.76	−3.39
CAC2235	*cysK*	Cysteine synthase/cystathionine beta-synthase	−1.05	2.79	4.37	8.49	1.54
CAC2542		FAD/FMN-containing dehydrogenase	1.93	2.20	1.82	1.93	5.73
CAC2543	*etfA*	Electron-transferring flavoprotein large subunit	1.97	2.06	1.76	1.76	4.79
CAC2544	*etfB*	Electron-transferring flavoprotein small subunit	1.82	1.52	2.20	1.90	5.15
CAC2746		Methyl-accepting chemotaxis protein	−3.42	n.d.	n.d.	n.d.	n.d.
CAC2774		Methyl-accepting chemotaxis protein	−4.84	−1.82	n.d.	n.d.	n.d.
CAC2963	*lacG*	6-Phospho-beta-D-galactosidase	14.38	13.90	17.83	1.23	21.63
CAC2964	*lacE*	PTS system lactose-specific enzyme IIBC	15.01	18.85	11.00	1.36	24.23
CAC2965	*lacF*	PTS system lactose-specific enzyme IIA	24.07	29.03	15.31	n.d.	34.72
CAC2966	*lacR*	Lactose phosphotransferase system repressor lacR	19.05	n.d.	17.65	2.20	n.d.
CAC3157	*trpA*	Tryptophan synthase alpha chain	−1.04	−4.11	−1.02	−97.96	31.04
CAC3158	*trpB*	Tryptophan synthase subunit beta	−1.00	−3.65	1.74	−61.58	35.21
CAC3159	*trpF*	Phosphoribosylanthranilate isomerase	1.02	−2.83	1.21	−133.66	28.93
CAC3160	*trpC*	Indole-3-glycerol phosphate synthase	1.04	−2.09	1.58	−91.00	40.81
CAC3161	*trpD*	Anthranilate phosphoribosyltransferase	1.02	−1.83	1.49	−178.59	38.79
CAC3162	*pabA*	*Para*-aminobenzoate synthase component II	−1.08	−1.76	1.69	−73.42	39.64
CAC3163	*parB*	Anthranilate synthase component I	1.20	−1.23	1.17	−151.59	36.19
CAC3388		Methyl-accepting chemotaxis protein	−3.29	n.d.	n.d.	n.d.	n.d.

RNA samples were drawn from steady-state acidogenic and solventogenic cells, respectively, as well as from cells during the late pH shift of the butyrate feeding experiment, and hybridized with corresponding wild-type RNA samples. Genes are listed in order of ORF numbers

ORF open reading frame, *n.d.* no ratio was calculated due to used filter criteria of the microarray

non-replicative plasmid, yielding strain PJC4BK (Green et al. 1996). In addition, antisense RNA strategies were employed against both the *buk* and the phosphotransbutyrylase-encoding *ptb* gene (Desai et al. 1999; Desai and Papoutsakis 1999). Despite the observation that a *buk* knockout or knockdown resulted in an enhanced butanol production, the recombinant strains still produced some butyrate (Desai et al. 1999). In contrast, the *ptb* knockdown strain *C. acetobutylicum* 824 (pRD1) revealed a poor solvent titer and produced primarily high amounts of acids, i.e., acetate, butyrate, and lactate (Desai and Papoutsakis 1999). More recently, the *ptb* gene was inactivated using a modified intron-based strategy without plasmid curing, but the acetate and butyrate levels of the resulting mutant *C. acetobutylicum* PKW were similar to those of the progenitor strain (Jang et al. 2012b). The first successful disruption of the *ptb* gene in *C. acetobutylicum* leading to a clear butyrate-negative phenotype was reported shortly before (Lehmann et al. 2012b). Another research group confirmed this noteworthy phenotype afterwards, also employing ClosTron mutagenesis, but a different target site of the *ptb* gene was chosen for the intron insertion (Cooksley et al. 2012). Both studies used batch cultures for phenotypic characterization of *ptb* mutants, and in both cases, high amounts of ethanol and lactate were observed, whereas butyrate was never detected during fermentation. Inactivation of the *hbd* gene, which encodes the 3-hydroxybutyryl-CoA dehydrogenase located upstream in the C_4 biosynthetic pathway, also altered the metabolic profile towards increased ethanol biosynthesis and neither butyrate nor butanol was produced (Lehmann and Lütke-Eversloh 2011).

In this study, the *ptb*::int(87) mutant cultivated in a phosphate-limited continuous culture exhibited a very

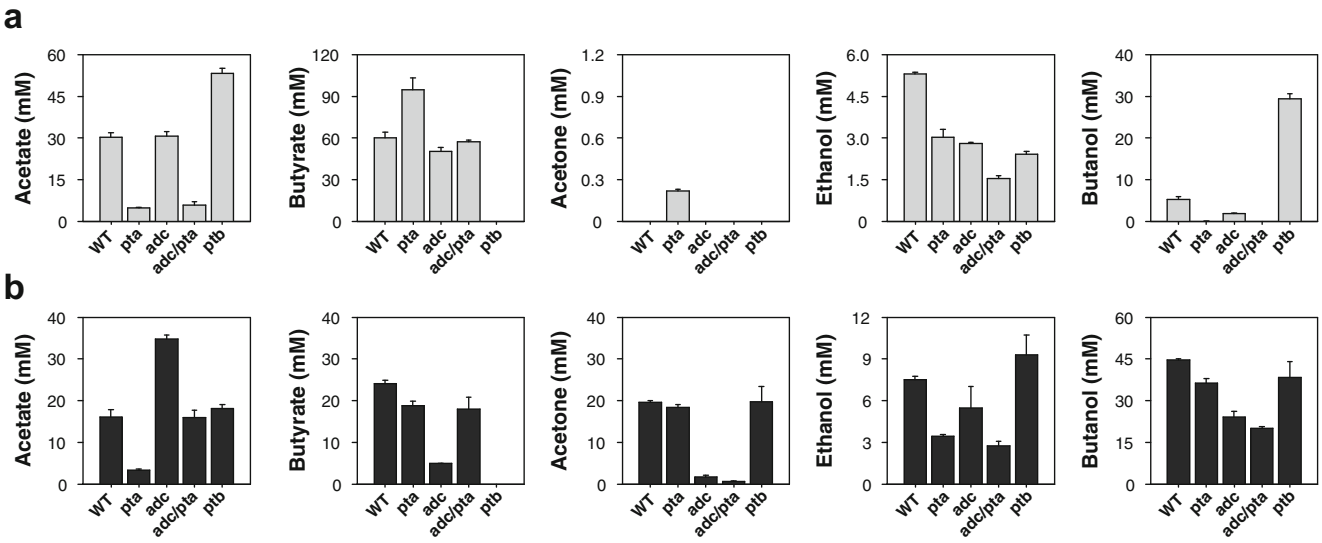

Fig. 5 Product patterns of all *C. acetobutylicum* strains analyzed in this study during steady-state acidogenic (**a**) and solventogenic (**b**) growth. *WT*, *C. acetobutylicum* ATCC 824; *pta*, *C. acetobutylicum pta*::int(80); *adc*, *C. acetobutylicum adc*::int(180); *adc/pta*, *C. acetobutylicum adc*::int(180)ΔRAM-*pta*::int(80); *ptb*, *C. acetobutylicum ptb*::int(87)

interesting product pattern with major differences to the batch cultures. Whereas the butyrate-negative phenotype and increased acetate concentrations were confirmed, ethanol was no longer a dominant product. No lactate was detectable during solventogenesis, and only small amounts (5–7 mM) were measured during acidogenesis as well as during the pH shift in the experiment where 20 mM butyrate was added to the feed medium. Acetone and ethanol levels were comparable to those of the parental wild type during steady-state solventogenic growth (Fig. 5). The most notable finding was that the *ptb* mutant produced significant quantities of butanol in the acidogenic growth phase at pH 5.7, challenging the long-lasting dogma that a low pH is an indispensable prerequisite for solvent biosynthesis in *C. acetobutylicum* (Bahl et al. 1982; Gottwald and Gottschalk 1985; Holt et al. 1984; Huang et al. 1985). According to the observed product pattern at pH 5.7 (production of butanol and ethanol but not acetone), it seems that the *ptb*::int(87) mutant has shifted to an alcohologenic metabolism. Beside the absence of acetone, this physiological condition is characterized among others by a decreased production of acids and an increased intracellular nicotinamide adenine dinucleotide (NADH)/NAD ratio (Fontaine et al. 2002; Girbal and Soucaille 1994; Peguin et al. 1994; Vasconcelos et al. 1994). Due to the missing butyrate formation, the *ptb* mutant exhibited a lower overall acid formation. An earlier shift to butanol production was already reported for some examples of engineered *C. acetobutylicum* strains growing in batch cultures (e.g., Scheel and Lütke-Eversloh 2013; Sillers et al. 2009; Wietzke and Bahl 2012). With the exception of a butyrate kinase mutant (*buk*) (Harris et al. 2000; Zhao et al. 2005), none of these strains showed a clear uncoupling of acidogenic and solventogenic growth or butanol formation during acidogenic growth. The interpretation of such batch fermentations is difficult due to responses to a changing growth rate or varying substrate and product concentrations. The chemostat cultures are ideally suited to separate the switch from acidogenesis to solventogenesis from those physiologically processes. To our best knowledge, this is the first report on the characterization of *C. acetobutylicum* mutant with a defect in the *ptb* using this fermentation technique.

The exergonic and irreversible decarboxylation of acetoacetate, catalyzed by the acetoacetate decarboxylase, which is encoded by the *adc* gene, has been described as a driving force during solventogenesis (Gheshlaghi et al. 2009; Jones and Woods 1986). However, acetone cannot be used as a biofuel, and therefore, it is the major unwanted by-product of ABE fermentation by *C. acetobutylicum*. In this respect, two metabolic engineering strategies were applied so far: (a) reduction of acetone to isopropanol by expression of a recombinant secondary alcohol dehydrogenase (Collas et al. 2012; Dai et al. 2012; Dusséaux et al. 2013; Jang et al. 2013a; Lee et al. 2012) and (b) reduced expression or disruption of the acetone biosynthetic genes. Although the expression of the *adc* gene was successfully downregulated by artificial antisense RNA constructs, no concomitant effect on acetone formation was observed (Tummala et al. 2003). To overcome the problem of transcriptional leakage that can occur during antisense RNA downregulation, the TargeTron technology was employed to inactivate the *adc* gene in the Chinese hyperbutanol-producing strain *C. acetobutylicum* EA 2018 (Jiang et al. 2009). The *adc*-negative mutant exhibited a drastically reduced acetone production, resulting in massive acetate accumulation and reduced butanol formation. Using the type strain *C. acetobutylicum* ATCC 824 and the ClosTron methodology, the mutant *C. acetobutylicum adc*::int(180) was generated which basically

exhibited a similar phenotype in batch fermentations (Lehmann et al. 2012a). These results were also confirmed by Cooksley et al. (2012), who generated strain Cac-*adc*180s::CT with the same mutagenesis system and the same intron insertion site in the *adc* gene. However, the fermentation profiles of the *adc*::int(180) mutant in continuous cultures were less pronounced in terms of acid accumulation because acetate and butyrate levels were comparable to the wild-type culture in the acidogenic phase at pH 5.7. In accordance with the batch cultures, very low concentrations of acetone were detected during solventogenic growth, and the butanol titer was reduced to approximately half of the wild-type concentration (Fig. 5). Spontaneous decarboxylation of acetoacetate is the most likely cause for the small amounts of acetone formed by the *adc* mutant. Furthermore, it was noticed that acetate was accumulated. This means that, in contrast to butyrate, reduced or no re-assimilation of acetate occurred. These observations support (i) the assumption of an acetoacetyl-CoA:acyl-CoA transferase (CtfAB) and Adc-dependent re-assimilation of acetate (Lee et al. 2008, 2009; Lehmann et al. 2012a; Sillers et al. 2008) and (ii) the idea that butyrate re-uptake is not necessarily related to acetone production in *C. acetobutylicum* (Jiang et al. 2009; Lehmann et al. 2012a, b).

Finally, the *adc*::int(180)ΔRAM-*pta*::int(80) double knockout mutant was subjected to continuous cultivation and exhibited the expected product pattern. Whereas butyrate was the main product during acidogenesis at pH 5.7, reduced amounts of butanol and ethanol were detected during solventogenesis at pH 4.5 in addition to the absence of acetone production, resulting in the lowest solvent titer of all mutant strains analyzed in this study (Fig. 5). A comparable phenotype could be observed for a *pta-ctfB*-deficient strain (CEKW) (Jang et al. 2012b). The distinct decline of the butyrate concentration again supported the assumption that butyrate was re-assimilated via an Adc/CtfAB-independent pathway in *C. acetobutylicum*.

In order to determine whether butyrate is mainly taken up via a Ptb/Buk-dependent pathway, butyrate feeding experiments were conducted with the butyrate-negative *ptb* mutant. In agreement with previous data (Lehmann et al. 2012b), the consumption of butyrate added to the medium indicated that butyrate uptake is independent of the *ptb* gene in *C. acetobutylicum* (Fig. 3b). Together with the observation that butyrate was clearly re-assimilated by a *ctfA*-negative mutant (Lehmann et al. 2012a), these findings raise the question of the nature of the butyrate uptake system.

In summary, the *pta* and *ptb* mutants with disrupted acid forming pathways were characterized more specifically under clearly defined continuous cultivation conditions revealing different product patterns from those described before for batch cultures, whereas the chemostat product profiles of the *adc* and *adc/pta* double mutants with inactivated acetoacetate decarboxylase genes were in good accordance with our previous data from batch cultures (Lehmann et al. 2012a, b).

The results of the DNA microarray analyses of genes of central metabolism in the mutants in comparison to wild-type expression levels are summarized in Tables 1 and 3. Most fermentative enzymes were not significantly regulated on the transcriptional level except for the *bcs* operon which was upregulated in the *ptb* and double knockout mutants during solventogenic growth, suggesting an elevated carbon flux towards butyryl-CoA.

The most striking expression changes were found for the *adhE2* gene (CAP0035), coding for a second NADH-dependent bifunctional aldehyde/alcohol dehydrogenase. While the *adhE2* gene was repressed in the *adc* mutant, the other three mutants exhibited up to two- or three-digit increases of *adhE2* transcripts. Interestingly, no corresponding increase in ethanol or butanol titers could be observed for these strains which suggest that CAP0035 is presumably not involved in alcohol production although overexpression of AdhE2 has been linked to the alcohologenic metabolism (Fontaine et al. 2002). While the exact regulatory mechanism is still unknown, a redox-dependent upregulation of *adhE2* is currently assumed (Fontaine et al. 2002; Hönicke et al. 2012; Wietzke and Bahl 2012). In *C. acetobutylicum*, CAP0035 is one of several operons that was found to be putative targets for Rex regulation (Wang et al. 2013). Rex, encoded by CAC2713, belongs to a family, which includes regulators that modulate transcription in response to cellular redox state (Ravcheev et al. 2012). However, a double knockout in terms of an additional insertion of the group II intron into the *rex* gene can be excluded, since all of the mutants analyzed in this study were screened by southern blotting (Lehmann et al. 2012a, b). Furthermore, the *rex*-negative strain described by Wietzke and Bahl (2012) exhibited a distinct phenotype with highly increased ethanol and reduced acetone production.

Another peculiar transcriptional pattern was observed for the pSOL1-encoded genes CAP0036 and CAP0037: whereas the expression was not significantly affected in the *adc* mutant, the *pta* mutant and the *adc/pta* double mutant revealed a clear induction during solventogenic growth at pH 4.5. In contrast, CAP0036 and CAP0037 were strongly repressed in the *ptb* mutant, regardless whether butyrate was added to the supplying medium or not (Table 4). The physiological role of these *ygaTS* orthologs of *Bacillus subtilis* is still unknown to date. In a recent study, the transcription of this uncharacterized operon was also found to be significantly regulated as response to metabolite stress (Wang et al. 2013). A putative function in transcriptional regulation related to the solventogenic shift was discussed (Schiel-Bengelsdorf et al. 2013). However, the appearance of CAP0036 and CAP0037 as distinct multiple spots in two-dimensional protein gels (Janssen et al. 2010; Schaffer et al. 2002) did not support this hypothesis. Hence, the function of CAP0036/CAP0037 in the metabolism of *C. acetobutylicum* remains to be elucidated.

All four mutant strains showed decreased expression levels of chemotaxis and motility genes, which was described for other clostridial mutants such as degenerated asporogenous strains as well (Paredes et al. 2005; Shi and Blaschek 2008; Tomas et al. 2003).

While the *pta* mutant showed lower transcript levels for genes of cysteine and methionine biosynthesis and related genes during acidogenic growth, these gene clusters were typically induced during solventogenic growth of the *pta*, *adc*, and *ptb* mutant strains but not significantly altered in the *adc/pta* double knockout strain (Tables 2 and 4). Considering the high butyrate concentrations in the *pta* mutant cultures at pH 5.7 as well as the acetate and butanol titers produced by the *ptb* mutant, these patterns fit to the results of Alsaker et al. (2010) who observed an upregulation of sulfur metabolic genes after acetate stress but a downregulation after butyrate exposure of *C. acetobutylicum*. Genes related to sulfur metabolism and transport were previously identified to be differentially expressed in analyses of *C. acetobutylicum* growing in continuous cultures (Grimmler et al. 2011) or in studies dealing with stress exposure experiments (Heluane et al. 2011; Janssen et al. 2012; Schwarz et al. 2012; Venkataramanan et al. 2013; Wang et al. 2013; Zhang and Ezeji 2013). Particularly, the large cluster CAC0102 to CAC0110 encoding genes for sulfate assimilation has several times been shown to be significantly regulated. A study by Wang et al. (2013) discussed that in *C. acetobutylicum*, the expression of genes involved in cysteine metabolism is controlled by the transcriptional regulator CymR. Based on orthology to the CymR target genes in *Bacillales* and *Staphylococcaceae*, they identified seven operons with potential CymR-binding sites in their promoter regions, including among others the operon CAC0102 to CAC0110. Thus, this characteristic group of open reading frames seems to play an essential role in the network of genes being involved in the sulfur metabolism.

Finally, two gene clusters were found to be significantly upregulated in the *ptb* mutant but not in the chemostat cultures of the other mutants. One of them, the *nif* cluster CAC0256 to CAC0261 encoding nitrogenase components, was highly induced in the *ptb* mutant, which was in accordance with recent studies employing acid and butanol stress to *C. acetobutylicum* (Alsaker et al. 2010; Janssen et al. 2012; Wang et al. 2013). The other cluster encoding the pyruvate formate lyase genes *pflAB* was significantly induced in the butyrate feeding experiment (Table 4). However, *C. acetobutylicum* neither possesses a formate dehydrogenase nor a formate hydrogen lyase, and formic acid has never been detected as a fermentation product. On the other hand, increased expression of the *pflAB* genes during growth has been described previously, and in addition, PflAB protein spots were measurable in proteome reference maps (Alsaker and Papoutsakis 2005; Janssen et al. 2010; Jones et al. 2008; Mao et al. 2010). Hence, the physiological function of the pyruvate formate lyase and its putative role in the one-carbon metabolism remains to be elucidated.

In conclusion, continuous cultivation and genome-wide DNA microarray analyses were demonstrated to be powerful and highly reproducible tools to analyze mutants of *C. acetobutylicum*. Application of these techniques can provide new insights into the physiology of genetically modified strains, taking into account recent reports on engineered *C. acetobutylicum* strains with interesting phenotypes (e.g., Jang et al. 2012b, 2013b; Mann and Lütke-Eversloh 2013; Scheel and Lütke-Eversloh 2013; Ventura et al. 2013).

Acknowledgments This study was financially supported by the German Federal Ministry of Education and Research (BMBF) through the COSMIC2 project no. 0315872D, Süd-Chemie AG (Munich, Germany), and the BMBF project no. 0315419A.

References

Alsaker KV, Papoutsakis ET (2005) Transcriptional program of early sporulation and stationary-phase events in *Clostridium acetobutylicum*. J Bacteriol 187:7103–7118

Alsaker KV, Paredes C, Papoutsakis ET (2010) Metabolite stress and tolerance in the production of biofuels and chemicals: gene-expression-based systems analysis of butanol, butyrate, and acetate stresses in the anaerobe *Clostridium acetobutylicum*. Biotechnol Bioeng 105:1131–1147

Bahl H, Andersch W, Braun K, Gottschalk G (1982) Effect of pH and butyrate concentration on the production of acetone and butanol by *Clostridium acetobutylicum* grown in continuous culture. Eur J Appl Microbiol Biotechnol 14:17–20

Berezina OV, Zakharova NV, Yarotsky CV, Zverlov VV (2012) Microbial producers of butanol. Appl Biochem Microbiol 48:625–638

Collas F, Kuit W, Clement B, Marchal R, Lopez-Contreras AM, Monot F (2012) Simultaneous production of isopropanol, butanol, ethanol and 2,3-butanediol by *Clostridium acetobutylicum* ATCC 824 engineered strains. AMB Express 2:45

Cooksley CM, Zhang Y, Wang H, Redl S, Winzer K, Minton NP (2012) Targeted mutagenesis of the *Clostridium acetobutylicum* acetone-butanol-ethanol fermentation pathway. Metab Eng 14:630–641

Dai Z, Dong H, Zhu Y, Zhang Y, Li Y, Ma Y (2012) Introducing a single secondary alcohol dehydrogenase into butanol-tolerant *Clostridium acetobutylicum* Rh8 switches ABE fermentation to high level IBE fermentation. Biotechnol Biofuels 5:44

Desai RP, Papoutsakis ET (1999) Antisense RNA strategies for metabolic engineering of *Clostridium acetobutylicum*. Appl Environ Microbiol 65:936–945

Desai RP, Harris LM, Welker NE, Papoutsakis ET (1999) Metabolic flux analysis elucidates the importance of the acid-formation pathways in regulating solvent production by *Clostridium acetobutylicum*. Metab Eng 1:206–213

Dusséaux S, Croux C, Soucaille P, Meynial-Salles I (2013) Metabolic engineering of *Clostridium acetobutylicum* ATCC 824 for the high-yield production of a biofuel composed of an isopropanol/butanol/ethanol mixture. Metab Eng 18:1–8

Ezeji T, Milne C, Price ND, Blaschek HP (2010) Achievements and perspectives to overcome the poor solvent resistance in acetone and butanol-producing microorganisms. Appl Microbiol Biotechnol 85:1697–1712

Fontaine L, Meynial-Salles I, Girbal L, Yang X, Croux C, Soucaille P (2002) Molecular characterization and transcriptional analysis of *adhE2*, the gene encoding the NADH-dependent aldehyde/alcohol dehydrogenase responsible for butanol production in alcohologenic cultures of *Clostridium acetobutylicum* ATCC 824. J Bacteriol 184: 821–830

Gheshlaghi R, Scharer JM, Moo-Young M, Chou CP (2009) Metabolic pathways of clostridia for producing butanol. Biotechnol Adv 27: 764–781

Girbal L, Soucaille P (1994) Regulation of *Clostridium acetobutylicum* metabolism as revealed by mixed-substrate steady-state continuous cultures: role of NADH/NAD ratio and ATP pool. J Bacteriol 176(21):6433–6438

Gottwald M, Gottschalk G (1985) The internal pH of *Clostridium acetobutylicum* and its effect on the shift from acid to solvent formation. Arch Microbiol 143:42–46

Green EM (2011) Fermentative production of butanol—the industrial perspective. Curr Opin Biotechnol 22:337–343

Green EM, Bennett GN (1996) Inactivation of an aldehyde/alcohol dehydrogenase gene from *Clostridium acetobutylicum* ATCC 824. Appl Biochem Biotechnol 57–58:213–221

Green EM, Boynton ZL, Harris LM, Rudolph FB, Papoutsakis ET, Bennett GN (1996) Genetic manipulation of acid formation pathways by gene inactivation in *Clostridium acetobutylicum* ATCC 824. Microbiology 142:2079–2086

Grimmler C, Janssen H, Kraubetae D, Fischer RJ, Bahl H, Dürre P, Liebl W, Ehrenreich A (2011) Genome-wide gene expression analysis of the Switch between acidogenesis and solventogenesis in continuous cultures of *Clostridium acetobutylicum*. J Mol Microbiol Biotechnol 20:1–15

Harris LM, Desai RP, Welker NE, Papoutsakis ET (2000) Characterization of recombinant strains of the *Clostridium acetobutylicum* butyrate kinase inactivation mutant: need for new phenomenological models for solventogenesis and butanol inhibition? Biotechnol Bioeng 67(1):1–11

Heap JT, Pennington OJ, Cartman ST, Carter GP, Minton NP (2007) The ClosTron: a universal gene knock-out system for the genus *Clostridium*. J Microbiol Methods 70:452–464

Heap JT, Kuehne SA, Ehsaan M, Cartman ST, Cooksley CM, Scott JC, Minton NP (2010) The ClosTron: mutagenesis in *Clostridium* refined and streamlined. J Microbiol Methods 80:49–55

Heluane H, Evans MR, Dagher SF, Bruno-Barcena JM (2011) Meta-analysis and functional validation of nutritional requirements of solventogenic Clostridia growing under butanol stress conditions and coutilization of D-glucose and D-xylose. Appl Environ Microbiol 77:4473–4485

Hillmann F, Fischer RJ, Saint-Prix F, Girbal L, Bahl H (2008) PerR acts as a switch for oxygen tolerance in the strict anaerobe *Clostridium acetobutylicum*. Mol Microbiol 68:848–860

Holt RA, Stephens GM, Morris JG (1984) Production of solvents by *Clostridium acetobutylicum* cultures maintained at neutral pH. Appl Environ Microbiol 48:1166–1170

Hönicke D, Janssen H, Grimmler C, Ehrenreich A, Lütke-Eversloh T (2012) Global transcriptional changes of *Clostridium acetobutylicum* cultures with increased butanol:acetone ratios. New Biotechnol 29:485–493

Huang L, Gibbins LN, Forsberg CW (1985) Transmembrane pH gradient and membrane potential in *Clostridium acetobutylicum* during growth under acetogenic and solventogenic conditions. Appl Environ Microbiol 50:1043–1047

Jang YS, Lee J, Malaviya A, Seung do Y, Cho JH, Lee SY (2012a) Butanol production from renewable biomass: rediscovery of metabolic pathways and metabolic engineering. Biotechnol J 7:186–198

Jang YS, Lee JY, Lee J, Park JH, Im JA, Eom MH, Lee J, Lee SH, Song H, Cho JH, Seung do Y, Lee SY (2012b) Enhanced butanol production obtained by reinforcing the direct butanol-forming route in *Clostridium acetobutylicum*. MBio 3:e00314-12

Jang YS, Malaviya A, Lee J, Im JA, Lee SY, Lee J, Eom MH, Cho JH, Seung do Y (2013a) Metabolic engineering of *Clostridium acetobutylicum* for the enhanced production of isopropanol-butanol-ethanol fuel mixture. Biotechnol Prog 29:1083–1088

Jang YS, Malaviya A, Lee SY (2013b) Acetone-butanol-ethanol production with high productivity using *Clostridium acetobutylicum* BKM19. Biotechnol Bioeng 110:1646–1653

Janssen H, Döring C, Ehrenreich A, Voigt B, Hecker M, Bahl H, Fischer RJ (2010) A proteomic and transcriptional view of acidogenic and solventogenic steady-state cells of *Clostridium acetobutylicum* in a chemostat culture. Appl Microbiol Biotechnol 87:2209–2226

Janssen H, Grimmler C, Ehrenreich A, Bahl H, Fischer RJ (2012) A transcriptional study of acidogenic chemostat cells of *Clostridium acetobutylicum*—solvent stress caused by a transient n-butanol pulse. J Biotechnol 161:354–365

Jiang Y, Xu C, Dong F, Yang Y, Jiang W, Yang S (2009) Disruption of the acetoacetate decarboxylase gene in solvent-producing *Clostridium acetobutylicum* increases the butanol ratio. Metab Eng 11:284–291

Jin C, Yao M, Liu H, Lee CFF, Ji J (2011) Progress in the production and application of n-butanol as a biofuel. Renew Sust Energ Rev 15: 4080–4106

Jones DT, Woods DR (1986) Acetone-butanol fermentation revisited. Microbiol Rev 50:484–524

Jones SW, Paredes CJ, Tracy B, Cheng N, Sillers R, Senger RS, Papoutsakis ET (2008) The transcriptional program underlying the physiology of clostridial sporulation. Genome Biol 9:R114

Kuit W, Minton NP, Lopez-Contreras AM, Eggink G (2012) Disruption of the acetate kinase (*ack*) gene of *Clostridium acetobutylicum* results in delayed acetate production. Appl Microbiol Biotechnol 94:729–741

Kumar M, Gayen K, Saini S (2013) Role of extracellular cues to trigger the metabolic phase shifting from acidogenesis to solventogenesis in *Clostridium acetobutylicum*. Bioresour Technol 138:55–62

Lee SY, Park JH, Jang SH, Nielsen LK, Kim J, Jung KS (2008) Fermentative butanol production by Clostridia. Biotechnol Bioeng 101:209–228

Lee JY, Jang YS, Lee J, Papoutsakis ET, Lee SY (2009) Metabolic engineering of *Clostridium acetobutylicum* M5 for highly selective butanol production. Biotechnol J 4:1432–1440

Lee J, Jang YS, Choi SJ, Im JA, Song H, Cho JH, Seung do Y, Papoutsakis ET, Bennett GN, Lee SY (2012) Metabolic engineering of *Clostridium acetobutylicum* ATCC 824 for isopropanol-butanol-ethanol fermentation. Appl Environ Microbiol 78:1416–1423

Lehmann D, Lütke-Eversloh T (2011) Switching *Clostridium acetobutylicum* to an ethanol producer by disruption of the butyrate/butanol fermentative pathway. Metab Eng 13:464–473

Lehmann D, Hönicke D, Ehrenreich A, Schmidt M, Weuster-Botz D, Bahl H, Lütke-Eversloh T (2012a) Modifying the product pattern of *Clostridium acetobutylicum*: physiological effects of disrupting the acetate and acetone formation pathways. Appl Microbiol Biotechnol 94:743–754

Lehmann D, Radomski N, Lütke-Eversloh T (2012b) New insights into the butyric acid metabolism of *Clostridium acetobutylicum*. Appl Microbiol Biotechnol 96:1325–1339

Liu S, Qureshi N (2010) How microbes tolerate ethanol and butanol. New Biotechnol 26:117–121

Lütke-Eversloh T (2014) Application of new metabolic engineering tools for *Clostridium acetobutylicum*. Appl Microbiol Biotechnol 98: 5823–5837

Lütke-Eversloh T, Bahl H (2011) Metabolic engineering of *Clostridium acetobutylicum*: recent advances to improve butanol production. Curr Opin Biotechnol 22:634–647

Maddox IS, Steiner E, Hirsch S, Wessner S, Gutierrez NA, Gapes JR, Schuster KC (2000) The cause of "acid-crash" and "acidogenic

fermentations" during the batch acetone-butanol-ethanol (ABE-) fermentation process. J Mol Microbiol Biotechnol 2:95–100

Mann MS, Lütke-Eversloh T (2013) Thiolase engineering for enhanced butanol production in *Clostridium acetobutylicum*. Biotechnol Bioeng 110:887–897

Mao S, Luo Y, Zhang T, Li J, Bao G, Zhu Y, Chen Z, Zhang Y, Li Y, Ma Y (2010) Proteome reference map and comparative proteomic analysis between a wild type *Clostridium acetobutylicum* DSM 1731 and its mutant with enhanced butanol tolerance and butanol yield. J Proteome Res 9:3046–3061

Nair RV, Green EM, Watson DE, Bennett GN, Papoutsakis ET (1999) Regulation of the sol locus genes for butanol and acetone formation in *Clostridium acetobutylicum* ATCC 824 by a putative transcriptional repressor. J Bacteriol 181(1):319–330

Nölling J, Breton G, Omelchenko MV, Makarova KS, Zeng Q, Gibson G, Hong Mei L, Dubois J, Qiu D, Hitti J, Aldredge T, Ayers M, Bashirzadeh R, Bochner H, Boivin M, Bross S, Bush D, Butler C, Caron A, Caruso A, Cook R, Daggett P, Deloughery C, Egan J, Ellston D, Engelstein M, Ezedi J, Gilbert K, Goyal A, Guerin J, Ho T, Holtham K, Joseph P, Keagle P, Kozlovsky J, LaPlante M, LeBlanc G, Lumm W, Majeski A, McDougall S, Mank P, Mao JI, Nocco D, Patwell D, Phillips J, Pothier B, Prabhakar S, Richterich P, Rice P, Rosetti D, Rossetti M, Rubenfield M, Sachdeva M, Snell P, Spadafora R, Spitzer L, Shimer G, Thomann HU, Vicaire R, Wall K, Wang Y, Weinstock K, Lai Peng W, Wonsey A, Xu Q, Zhang L, Wolf YI, Tatusov RL, Sabathe F, Doucette-Stamm L, Soucaille P, Daly MJ, Bennett GN, Koonin EV, Smith DR (2001) Genome sequence and comparative analysis of the solvent-producing bacterium *Clostridium acetobutylicum*. J Bacteriol 183:4823–4838

Papoutsakis ET (2008) Engineering solventogenic clostridia. Curr Opin Biotechnol 19:420–429

Paredes CJ, Alsaker KV, Papoutsakis ET (2005) A comparative genomic view of clostridial sporulation and physiology. Nat Rev Microbiol 3: 969–978

Peguin S, Goma G, Delorme P, Soucaille P (1994) Metabolic flexibility of *Clostridium acetobytylicum* in response to methyl viologen addition. Appl Microbiol Biotechnol 42(4):611–616

Ravcheev DA, Li X, Latif H, Zengler K, Leyn SA, Korostelev YD, Kazakov AE, Novichkov PS, Osterman AL, Rodionov DA (2012) Transcriptional regulation of central carbon and energy metabolism in bacteria by redox-responsive repressor Rex. J Bacteriol 194(5): 1145–1157

Roos JW, McLaughlin JK, Papoutsakis ET (1985) The effect of pH on nitrogen supply, cell lysis, and solvent production in fermentations of *Clostridium acetobutylicum*. Biotechnol Bioeng 27:681–694

Schaffer S, Isci N, Zickner B, Dürre P (2002) Changes in protein synthesis and identification of proteins specifically induced during solventogenesis in *Clostridium acetobutylicum*. Electrophoresis 23(1):110–121

Scheel M, Lütke-Eversloh T (2013) New options to engineer biofuel microbes: development and application of a high-throughput screening system. Metab Eng 17:51–58

Schiel-Bengelsdorf B, Montoya J, Linder S, Dürre P (2013) Butanol fermentation. Environ Technol 34:1691–1710

Schwarz KM, Kuit W, Grimmler C, Ehrenreich A, Kengen SW (2012) A transcriptional study of acidogenic chemostat cells of *Clostridium acetobutylicum*—cellular behavior in adaptation to n-butanol. J Biotechnol 161:366–377

Shi Z, Blaschek HP (2008) Transcriptional analysis of *Clostridium beijerinckii* NCIMB 8052 and the hyper-butanol-producing mutant BA101 during the shift from acidogenesis to solventogenesis. Appl Environ Microbiol 74:7709–7714

Sillers R, Chow A, Tracy B, Papoutsakis ET (2008) Metabolic engineering of the non-sporulating, non-solventogenic *Clostridium acetobutylicum* strain M5 to produce butanol without acetone demonstrate the robustness of the acid-formation pathways and the importance of the electron balance. Metab Eng 10:321–332

Sillers R, Al-Hinai MA, Papoutsakis ET (2009) Aldehyde-alcohol dehydrogenase and/or thiolase overexpression coupled with CoA transferase downregulation lead to higher alcohol titers and selectivity in *Clostridium acetobutylicum* fermentations. Biotechnol Bioeng 102: 38–49

Tashiro Y, Yoshida T, Noguchi T, Sonomoto K (2013) Recent advances and future prospects for increased butanol production by acetone-butanol-ethanol fermentation. Eng Life Sci 13:432–445

Thormann K, Feustel L, Lorenz K, Nakotte S, Dürre P (2002) Control of butanol formation in *Clostridium acetobutylicum* by transcriptional activation. J Bacteriol 184:1966–1973

Tomas CA, Alsaker KV, Bonarius HP, Hendriksen WT, Yang H, Beamish JA, Paredes CJ, Papoutsakis ET (2003) DNA array-based transcriptional analysis of asporogenous, nonsolventogenic *Clostridium acetobutylicum* strains SKO1 and M5. J Bacteriol 185:4539–4547

Tummala SB, Welker NE, Papoutsakis ET (2003) Design of antisense RNA constructs for downregulation of the acetone formation pathway of *Clostridium acetobutylicum*. J Bacteriol 185:1923–1934

Vasconcelos I, Girbal L, Soucaille P (1994) Regulation of carbon and electron flow in *Clostridium acetobutylicum* grown in chemostat culture at neutral pH on mixtures of glucose and glycerol. J Bacteriol 176(5):1443–1450

Venkataramanan KP, Jones SW, McCormick KP, Kunjeti SG, Ralston MT, Meyers BC, Papoutsakis ET (2013) The *Clostridium* small RNome that responds to stress: the paradigm and importance of toxic metabolite stress in *C. acetobutylicum*. BMC Genomics 14: 849

Ventura JR, Hu H, Jahng D (2013) Enhanced butanol production in *Clostridium acetobutylicum* ATCC 824 by double overexpression of 6-phosphofructokinase and pyruvate kinase genes. Appl Microbiol Biotechnol 97:7505–7516

Wang S, Zhang Y, Dong H, Mao S, Zhu Y, Wang R, Luan G, Li Y (2011) Formic acid triggers the "acid crash" of acetone-butanol-ethanol fermentation by *Clostridium acetobutylicum*. Appl Environ Microbiol 77:1674–1680

Wang Q, Venkataramanan KP, Huang H, Papoutsakis ET, Wu CH (2013) Transcription factors and genetic circuits orchestrating the complex, multilayered response of *Clostridium acetobutylicum* to butanol and butyrate stress. BMC Syst Biol 7:120

Wiesenborn DP, Rudolph FB, Papoutsakis ET (1988) Thiolase from *Clostridium acetobutylicum* ATCC 824 and its role in the synthesis of acids and solvents. Appl Environ Microbiol 54:2717–2722

Wietzke M, Bahl H (2012) The redox-sensing protein Rex, a transcriptional regulator of solventogenesis in *Clostridium acetobutylicum*. Appl Microbiol Biotechnol 96:749–761

Zhang Y, Ezeji TC (2013) Transcriptional analysis of *Clostridium beijerinckii* NCIMB 8052 to elucidate role of furfural stress during acetone butanol ethanol fermentation. Biotechnol Biofuels 6: 66

Zhao Y, Tomas CA, Rudolph FB, Papoutsakis ET, Bennett GN (2005) Intracellular butyryl phosphate and acetyl phosphate concentrations in *Clostridium acetobutylicum* and their implications for solvent formation. Appl Environ Microbiol 71(1):530–537